Synthesis and Evaluation in Monkey of Two Sensitive ^{11}C-Labeled Aryloxyanilide Ligands for Imaging Brain Peripheral Benzodiazepine Receptors In Vivo

Emmanuelle Briard, Sami S. Zoghbi, Masao Imaizumi, Jonathan P. Gourley, H. Umesha Shetty, Jinsoo Hong, Vanessa Cropley, Masahiro Fujita, Robert B. Innis, and Victor W. Pike*

Molecular Imaging Branch, National Institute of Mental Health, National Institutes of Health, Building 10, Room B3 C346A, 10 Center Drive, Bethesda, Maryland 20892

Received June 22, 2007

We sought to develop ^{11}C-labeled ligands for sensitive imaging of brain peripheral benzodiazepine receptors (PBR) in vivo. Two aryloxyanilides with high affinity for PBR were identified and synthesized, namely, *N*-acetyl-*N*-(2-methoxycarbonylbenzyl)-2-phenoxyaniline (**3**, PBR01) and *N*-(2-methoxybenzyl)-*N*-(4-phenoxypyridin-3-yl)acetamide (**10**, PBR28). **3** was hydrolyzed to **4**, which was esterified with [^{11}C]iodomethane to provide [^{11}C]**3**. The *O*-desmethyl analogue of **10** was converted into [^{11}C]**10** with [^{11}C]iodomethane. [^{11}C]**3** and [^{11}C]**10** were each injected into monkey to assess their brain kinetics with positron emission tomography (PET). After administration of either radioligand there was moderately high brain uptake of radioactivity. Receptor blocking and displacement experiments showed that a high proportion of this radioactivity was bound specifically to PBR. In monkey and rat, **3** and **10** were rapidly metabolized by ester hydrolysis and N-debenzylation, respectively, each to a single polar radiometabolite. [^{11}C]**3** and [^{11}C]**10** are effective for imaging PBR in monkey brain. [^{11}C]**10** especially warrants further evaluation in human subjects.

Introduction

The "peripheral benzodiazepine receptor" (PBR[a]), recently called the "translocator protein (18 kDa)",[1] is wholly distinct structurally, functionally, and pharmacologically from the well-known classes of brain receptors that bind both GABA and synthetic benzodiazepines (e.g., diazepam). Originally discovered as a diazepam binding site in kidney,[2] PBR is an evolutionarily well-conserved and highly hydrophobic 18 kDa protein that is associated with the voltage-dependent ion channel and adenine nucleotide transporter at the contact site between outer and inner mitochondrial membranes.[3] PBRs are also expressed on plasma membranes in erythrocytes.[4] At mitochondria, the PBR protein is arranged in five transmembrane domains[5] forming a cavity that likely contributes to a permeability transition core.[6] PBRs have many putative functions, such as cholesterol transport from the outer to inner mitochondrial membrane[7,8] and involvement in regulation of cell death,[3] cell proliferation,[9] and ion transport.[10,11] PBRs are widely distributed throughout the body.[12] The glands and gonads are particularly rich, while the kidney, lung, and heart have intermediate levels, and the liver and brain have low levels.

PBRs are implicated in numerous nervous system disorders such as epilepsy, cerebral ischemia, astrocytoma, nerve injury, and neurodegenerative diseases.[13,14] Brain PBR density increases in several neuropathological conditions and also after experimental injuries to the central nervous system.[15] Evidence suggests that these increases are mainly associated with activated microglia and to a lesser extent with astrocytes. The prototypical PBR-selective radioligand, the isoquinoline carboxamide [^{11}C]PK 11195, initially as its racemate[16] and later as its single *R*-enantiomer[17] (Figure 1), has long been used with positron emission tomography (PET) to visualize such changes in vivo (for a recent comprehensive review, see Venneti et al.[18]). Examples include imaging of elevated PBR in dementia,[19] herpes encephalitis,[20] and multiple sclerosis.[21,22] Nonetheless, [^{11}C]PK 11195 has many limitations on its sensitivity and accuracy for measuring PBR increases. In human subjects these include low brain uptake,[22] low sensitivity (i.e., a low ratio of PBR-specific to nonspecific binding), extensive metabolism to several unidentified less lipophilic radiometabolites,[23–25] that have a possible undesirable ability to enter brain, and finally

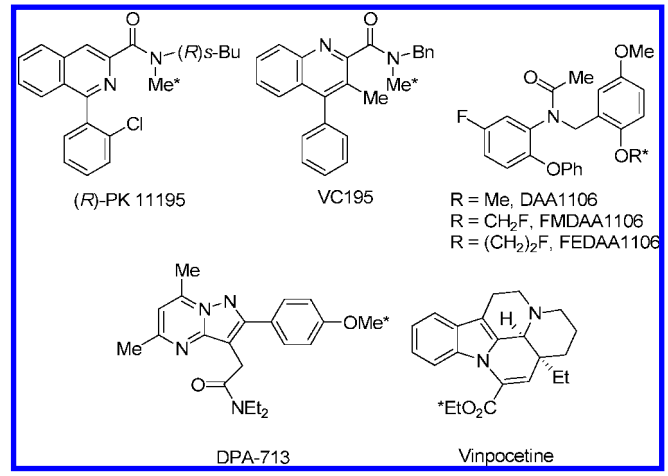

Figure 1. Structures of some PBR ligands. Asterisks mark positions in which ligands have been labeled with either carbon-11 or fluorine-18.

* To whom correspondence should be addressed. Phone: 301-594-5986. Fax: 301-480-5112. E-mail: pikev@mail.nih.gov.

[a] Abbreviations: D, dopaminergic; DAA1106, *N*-(2,5-dimethoxybenzyl)-*N*-(5-fluoro-2-phenoxyphenyl)acetamide; DAT, dopamine transporter; EOS, end of synthesis; ERP, end of radionuclide production; FDA, Food and Drug Administration; [^{18}F]FEDAA1106, *O*-[^{18}F]2-(2-fluoroethyl)desmethyl-DAA1106; [^{18}F]FMDAA1106, *O*-[^{18}F]2-fluoromethyldesmethyl-DAA1106; GABA, γ-aminobutyric acid; H, histaminergic; HEPES, 4-(2-hydroxyethyl)piperazineethanesulfonic acid; IND, investigational new drug; M, muscarinic; PET, positron emission tomography; PBR, peripheral benzodiazepine receptor; PK 11195, 1-(2-chlorophenyl)-*N*-methyl-*N*-(1-methylpropyl)-3-isoquinoline carboxamide; RCY, decay-corrected radiochemical yield; NET, noradrenaline transporter; rt, room temperature; SERT, serotonin transporter; SR, specific radioactivity; SUV, standardized uptake value; 5-HT, serotonin.

10.1021/jm0707370
Published on Web 12/08/2007

variable binding to blood proteins.[26] [^{11}C]PK 11195 shows similarly moderate brain uptake, low sensitivity, and extensive metabolism in animals (mouse,[23] rat,[27] pig,[28] baboon,[29] and rhesus monkey[30]). All these factors contribute to difficulty in robustly quantifying regional variations in PBR density in human and animal subjects with [^{11}C]PK 11195; therefore, sophisticated biomathematical efforts have become necessary to try to surmount these issues with this radioligand.[31–33]

Recently, new structural classes of high-affinity PBR ligands have been discovered, opening up opportunities for developing improved PET radioligands for PBR. These include quinoline carboxamides, benzothiazepines, benzoxazepines, indoleacetamides, pyrazolopyrimidines, vinca alkaloids, and aryloxyanilides.[34] Subsequently, many candidate PBR radioligands for PET imaging have been proposed and assessed in animals, including [^{11}C]DAA1106,[35–37] [^{18}F]FMDAA1106,[38,39] [^{18}F]FEDAA1106,[38,39] [^{11}C]DPA-713,[40] [^{11}C]VC195,[41] and [^{11}C]vinpocetine[42] (Figure 1). Although some of these radioligands appear promising, for many of them data in human subjects are so far sparse or nonexistent and preclude a final conclusion on their utility for measuring PBR in clinical situations. Exceptionally, two of the more promising PET radioligands, based on aryloxyanilides, have very recently entered study in human subjects, namely, [^{11}C]DAA1106[43] and [^{18}F]FEDAA1106.[44] Even so, these radioligands may turn out to have less than ideal kinetic properties that ultimately limit their effective application for quantitative studies. We have sought to develop alternative sensitive brain-penetrant PBR ligands from the aryloxyanilide class, as we now report here.

Specifically, we report the radiosyntheses and evaluations of ^{11}C-labeled versions of an especially high-affinity ligand, namely, *N*-acetyl-*N*-(2-methoxycarboxybenzyl)-2-phenoxyaniline (**3**, PBR01) (IC_{50} = 0.0643 nM)[45] and another less lipophilic alternative, namely, *N*-(2-methoxybenzyl)-*N*-(4-phenoxypyridin-3-yl)acetamide (**10**, PBR28) (IC_{50} = 0.658 nM).[46] Ligands were simply labeled by alkylation of a prepared desmethyl precursor with [^{11}C]iodomethane, itself generated from cyclotron-produced [^{11}C]carbon dioxide. The PBR binding affinities in rat, monkey, and human tissue homogenates, brain uptake and distribution in vivo, and metabolite analysis of [^{11}C]**3** and [^{11}C]**10** are reported here. [^{11}C]**3** and [^{11}C]**10** are each found to be sensitive radioligands for imaging PBR in monkey brain, and [^{11}C]**10** in particular poses high potential for measuring PBR in human subjects with PET.

Results

Chemistry. Ligands **3** and **10** were obtained efficiently and in useful yields from commercial materials based on general synthetic methods[45,46] (Schemes 1 and 2). Ligand **3** was converted by simple hydrolysis into the acid precursor **4** that was required for the synthesis of [^{11}C]**3** (Scheme 1). The phenol precursor **13** required for the synthesis of [^{11}C]**10** was prepared de novo in three steps from commercial materials (Scheme 3). Metabolite **8** was obtained by simple acetylation of the amine **7** with acetyl chloride.

Ligand Pharmacological Assays and Screen. The affinities of ligand **3** for PBR in rat, monkey, and human mitochondrial fractions were high and similar to those of DAA1106, while those of ligand **10** were marginally lower, especially for rat tissue (Table 1). The affinity of PK 11195 was significantly lower than for the aryloxyanilides in monkey and human. Ligands **3**, **10**, and DAA1106 all showed a small interspecies variability in affinity for PBR, with that for human tissue being somewhat lower than for monkey or rat. Values for the affinities of ligands **3**, **10**, and DAA1106 for rat tissue PBR were broadly consistent with those previously found.[45,46] Ligand **10** showed a K_i of >10 μM at several central benzodiazepine ($GABA_A$) receptors ($\alpha_1\beta_1\gamma_2$, $\alpha_2\beta_2\gamma_2$, $\alpha_5\beta_2\gamma_2$, and $\alpha_6\beta_2\gamma_2$ subtypes) and at 10 μM concentration was found to cause less than 50% displacement of reference ligand from 5-$HT_{1A,1B,1D,1E,2A-C,3,5A,6,7}$, $\alpha_{1A,1B,2A-C}$, β_{1-3}, D_{1-4}, H_{1-4}, $M_{2,5}$, DAT, NET, and SERT sites. A full displacement study revealed a K_i of 2.2 μM at κ opiate receptors.

Computation of cLogD and cLogP and Measurement of LogD. The measured LogD values and computed cLogP and cLogD values of **3**, **10**, and PK 11195 are shown in Table 1.

Scheme 1. Synthesis of Ligand **3**, Precursor **4**, and Radioligand [^{11}C]**3** [a]

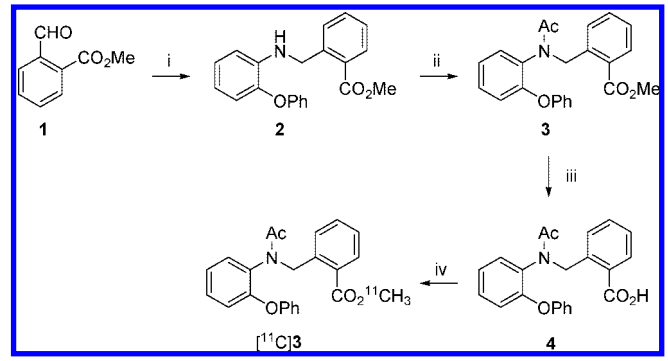

[a] Reagents, conditions, and yields: (i) 2-phenoxyaniline, MeOH, rt, 24 h, then $NaBH_4$, rt, 1 h, yield 65%; (ii) MeCOCl, Et_3N, CH_2Cl_2, rt, 1 h, yield 71%; (iii) KOH, MeOH, rt, 1 h, yield 85%; (iv) DMF, (^{t}Bu)$_4$NOH, MeOH, $^{11}CH_3I$, rt, ~9 min, RCY 18% from [^{11}C]carbon dioxide.

Scheme 2. Synthesis of Ligand **10** and Metabolite **8** [a]

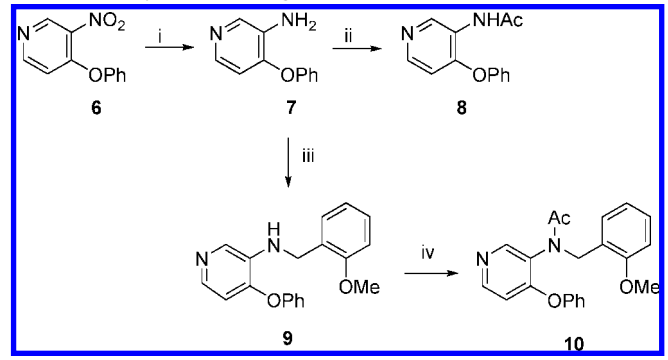

[a] Reagents, conditions, and yields: (i) Fe powder, HCl in aqueous EtOH, reflux, 3 h, 74%; (ii) AcCl, Et_3N, CH_2Cl_2, rt, 1 h, 55%; (iii) 2-methoxybenzaldehyde, toluene, reflux, 24 h, then $NaBH_4$, MeOH, rt, 1 h, 90%; (iv) Ac_2O, AcOH, reflux, 2 h, 84%.

Scheme 3. Synthesis of Phenol Precursor **13** and [^{11}C]**10** [a]

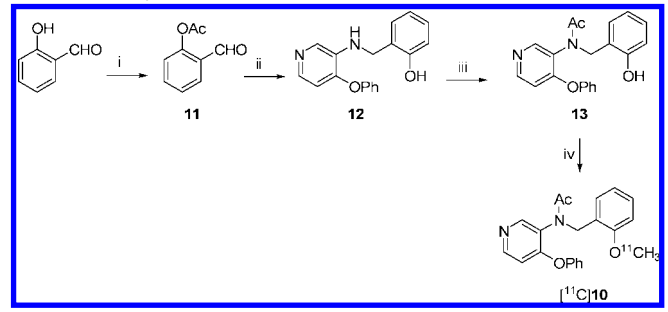

[a] Reagents, conditions, and yields: (i) Ac_2O, pyridine, rt, overnight, 95%; (ii) **7**, toluene, reflux, 24 h, then $NaBH_4$, MeOH, reflux, 3 h, 25%; (iii) Ac_2O, AcOH, reflux, 3 h, then KOH, MeOH, rt, 3 h, 63%; (iv) (^{t}Bu)$_4$NOH, MeOH, $^{11}CH_3I$, rt, ~7 min, RCY 25% from [^{11}C]carbon dioxide.

Table 1. PBR Lipophilicity, Affinity, Blood Distribution, and Free Fraction (f_P) Data for [^{11}C]**3**, [^{11}C]**10**, DA1106, and [^{11}C]PK 11195

radioligand	cLogP	cLogD	LogD[a]	K_i for PBR (nM)	monkey plasma: cell distribution (%)	monkey f_P (%)
[^{11}C]**3**	4.4	4.4	3.90 ± 0.02	1.40 ± 0.07[b] 0.254 ± 0.009[d] 0.0978 ± 0.0058[e]	36.7 ± 4.0: 63.3 ± 4.0[c]	0.15 ± 0.06[c]
[^{11}C]**10**	3.01	2.95	3.01 ± 0.11	2.47 ± 0.39[b] 0.944 ± 0.101[d] 0.680 ± 0.027[e]	33.2 ± 2.1: 66.8 ± 2.1[f]	5.6 ± 0.1[g]
DAA1106	4.28	4.28	nd[h]	0.242 ± 0.016[b] 0.230 ± 0.011[d] 0.0726 ± 0.0036[e]	nd[h]	nd[h]
[^{11}C]PK 11195	5.28	5.28	3.97 ± 0.18	4.50 ± 0.43[b] 4.35 ± 0.52[d] 0.73 ± 0.05[e]	nd[h]	nd[h]

[a] Mean ± SD for six determinations. [b] For human mitochondrial tissue; mean ± SD for six determinations. PK 11195 was found to have a K_D of 5.17 ± 3.00 nM ($n = 6$) in this assay. [c] Mean ± SD for four determinations. [d] For monkey mitochondrial tissue; mean ± SD for six determinations. PK 11195 was found to have a K_D of 3.48 ± 1.26 nM ($n = 6$) in this assay. [e] For rat mitochondrial tissue; mean ± SD for six determinations. PK 11195 was found to have a K_D of 0.707 ± 0.361 nM ($n = 6$) in this assay. [f] Mean ± SD for three determinations. [g] Mean ± SD for nine determinations. [h] nd = not determined.

Ligand **10** shows the lower values. Ligands **3** and PK 11195 were found to have similar measured LogD values. The cLogD value of the acid **15** was found to be −1.52.

Synthesis of Radioligands. [^{11}C]**3** and [^{11}C]**10** were readily prepared in acceptable isolated and formulated decay-corrected radiochemical yields from cyclotron-produced [^{11}C]carbon dioxide (18% and 26%, respectively), and in high chemical and radiochemical purity (>99%), with specific radioactivity (SR) in the range 2.04−3.73 Ci/μmol for [^{11}C]**3** and 2.28−8.90 Ci/μmol for [^{11}C]**10** at EOS (end of synthesis) (about 30 min from the start of radiosynthesis). The formulated radioligands were radiochemically stable for at least 1 h.

Analysis of Radioligand Distribution in Monkey Blood. The monkey blood distribution and plasma free fraction (f_P) values of [^{11}C]**3** and [^{11}C]**10** are presented in Table 1. Both radioligands were distributed mainly to cellular blood elements. [^{11}C]**10** has a much higher f_P value than [^{11}C]**3**.

Stability of Radioligands in Whole Monkey Blood, Rat Brain Homogenate, and Buffer. Radio-HPLC analysis of radioactivity extracted from monkey plasma incubated with either [^{11}C]**3** or [^{11}C]**10** for >30 min showed [^{11}C]**3** and [^{11}C]**10** to be 96.5 ± 1.5% ($n = 5$) and 95.8 ± 1.6% ($n = 10$) unchanged, respectively. [^{11}C]**10** was 99.8% unchanged after incubation with rat brain homogenate in saline for 2 h at 37 °C. After 2.5 h of storage in sodium phosphate buffer (0.15 M, pH 7.4), [^{11}C]**3** and [^{11}C]**10** were 99.9 ± 0.0% ($n = 4$) and 99.0 ± 0.2% ($n = 4$) unchanged, respectively.

Monkey PET Imaging Experiments. After injection of [^{11}C]**3** into monkey, radioactivity entered the brain well with peak uptake occurring in all PBR-containing regions at later than 10 min after injection (Figure 2A). Maximal uptake was 259% SUV in choroid plexus of fourth ventricle. The washout of radioactivity from all PBR-containing regions was quite slow. In an experiment in which PBR receptors were blocked in the same monkey by coadministration of **3**, the kinetics of brain radioactivity was strikingly different. Radioactivity was rapidly taken into all examined brain regions and to a much higher level than in the baseline experiment and then rapidly washed out (Figure 2B). In a displacement experiment, radioactivity in all PBR-containing regions was substantially reduced after administration of PK 11195 (Figure 2C).

In a baseline experiment in the same monkey, [^{11}C]**10** behaved similarly to [^{11}C]**3** except that maximal brain radioactivity uptake was higher (394% SUV in choroid plexus of fourth ventricle) (Figure 3A). In another experiment with [^{11}C]**10** in the same monkey, in which PBR receptors were preblocked with DAA1106, the kinetics of brain radioactivity was again strikingly different. Radioactivity was rapidly taken into all examined brain regions and to a higher level than in the baseline experiment and then rapidly washed out to a low level (Figure 3B). In an experiment in which PK 11195 was used as displacing agent, radioactivity in all PBR-containing regions was rapidly and substantially reduced (Figure 3C).

Figure 4 shows PET summation images of monkey brains acquired over a late period after injection of either [^{11}C]**3** (summed between 100 and 150 min) or [^{11}C]**10** (summed between 80 and 120 min) and coregistered with MRI scans. Each radioligand displays a high level of radioactivity in brain especially in the cerebellum, striatum, and choroid plexus of the fourth ventricle and displays intermediate levels in frontal, parietal, temporal, and occipital regions.

Emergence of Radiometabolites in Monkey Blood In Vivo. During PET experiments with [^{11}C]**3** and [^{11}C]**10**, recoveries of radioactivity from plasma into supernatant acetonitrile for HPLC analysis averaged 91.0 ± 6.8% ($n = 30$) and 95.8 ± 3.3% ($n = 27$), respectively. [^{11}C]**3** gave only one radiometabolite in plasma that eluted at the void volume on reverse-phase HPLC ($t_R = 2.1 \pm 0.1$ min; $n = 29$), as did [^{11}C]**10** (radiometabolite $t_R = 2.0 \pm 0.4$ min; $n = 22$), while the parent radioligands eluted in the same analyses at 4.7 ± 0.7 and 3.9 ± 0.7 min, respectively.

Figure 5 shows the time course of radioactive species in plasma after injection of monkey with [^{11}C]**3** in the baseline and self-block experiments. The time at which plasma radioactivity was composed equally of parent radioligand and radiometabolite was significantly shorter in the self-block experiment (8.2 min) than in the baseline experiment (20.2 min). A similar pattern was seen for [^{11}C]**10** between the preblock and baseline experiments (Figure 6).

For [^{11}C]**3**, the level of parent radioligand in plasma (% SUV) was substantially higher in the self-block than in the baseline experiment, especially over the initial 6 min; peak values were nearly 7-fold higher in the self-block experiment (Figure 7). A similar pattern was also shown by [^{11}C]**10** between the preblock and baseline experiments (Figure 8).

Radiometabolites in Rat Plasma, Urine, and Brain In Vivo. At 30 min after administration of either [^{11}C]**3** or [^{11}C]**10** to rat, recoveries of radioactivity from plasma, urine, and brain homogenate samples into supernatant acetonitrile for analysis with reverse-phase radio-HPLC were generally very high (values are shown in parentheses in Table 2). Recoveries of injected radioactivity from HPLC were quantitative in all cases. For each radioligand in all samples, HPLC analyses revealed a single polar radiometabolite for [^{11}C]**3** ($t_R = 2.1$ min) and for [^{11}C]**10** ($t_R = 2.2$ min) (cf. $t_R = 4.8$, and 6.5 min for [^{11}C]**3** and [^{11}C]**10**, respectively). In brain, in each case, parent radioligand was predominant, while in plasma and urine, radiometabolite was predominant (Table 2). With reduction of the amount of carrier in experiments with [^{11}C]**10**, the percentage of radioactivity in brain represented by unchanged radioligand increased (Table 2). In an experiment with [^{11}C]**10** in a rat that was perfused with saline during sacrifice, the level of radioactivity represented by unchanged radioligand (95.2%) was high and fully consistent with that seen in nonperfused rats.

LC−MS, MS−MS, and GC−MS of Reference Compounds. LC−MS of ligand **3** ($t_R = 14.76$ min) gave the protonated molecule ($[M + H]^+$, m/z 376) and fragment ions

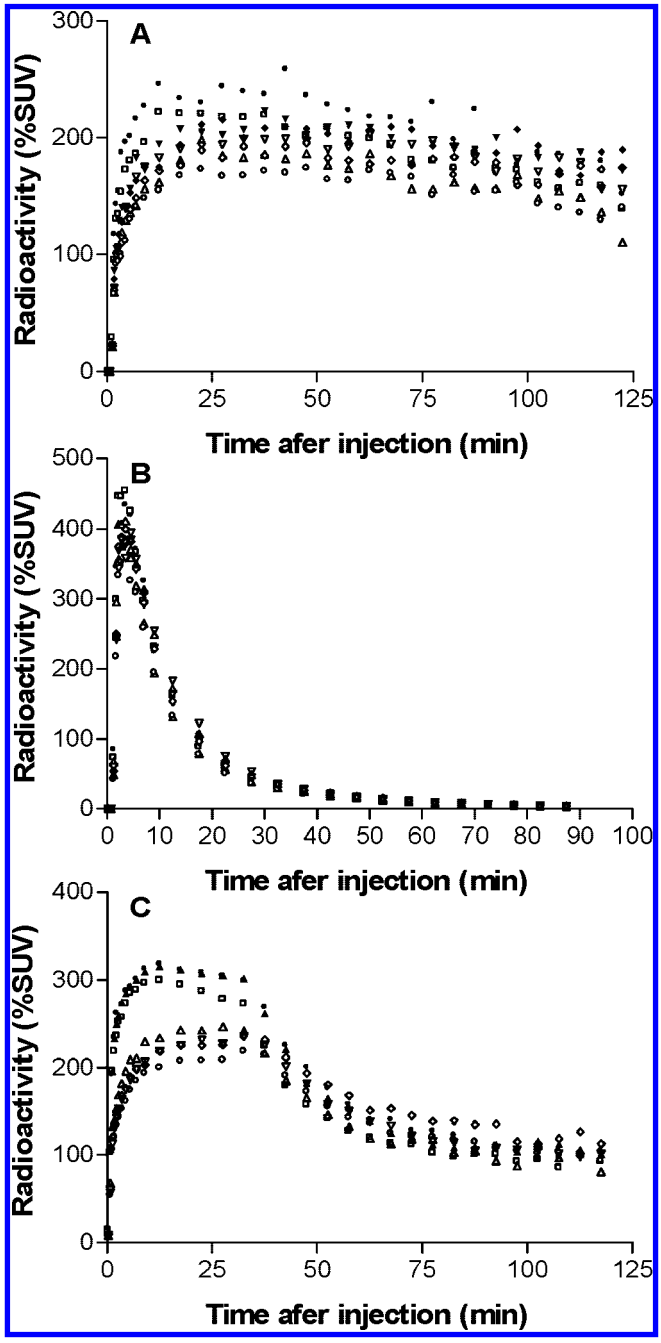

Figure 2. Brain region time-activity curves (TACs) in rhesus monkey after injection of [^{11}C]**3** alone (baseline experiment) (A), after injection of **3** with [^{11}C]**3** (self-block experiment) (B), and after injection of [^{11}C]**3** and then PK 11195 at 45 min later (displacement experiment) (C). Experiments in parts A and B were performed in the same monkey (and the same monkey giving the data shown in parts A and B of Figure 3): □, cerebellum; △, occipital cortex; ▽, parietal cortex; ◇, temporal cortex; ○, frontal cortex; ◆, putamen; ▼, thalamus; ▲, striatum; ●, choroid plexus of fourth ventricle.

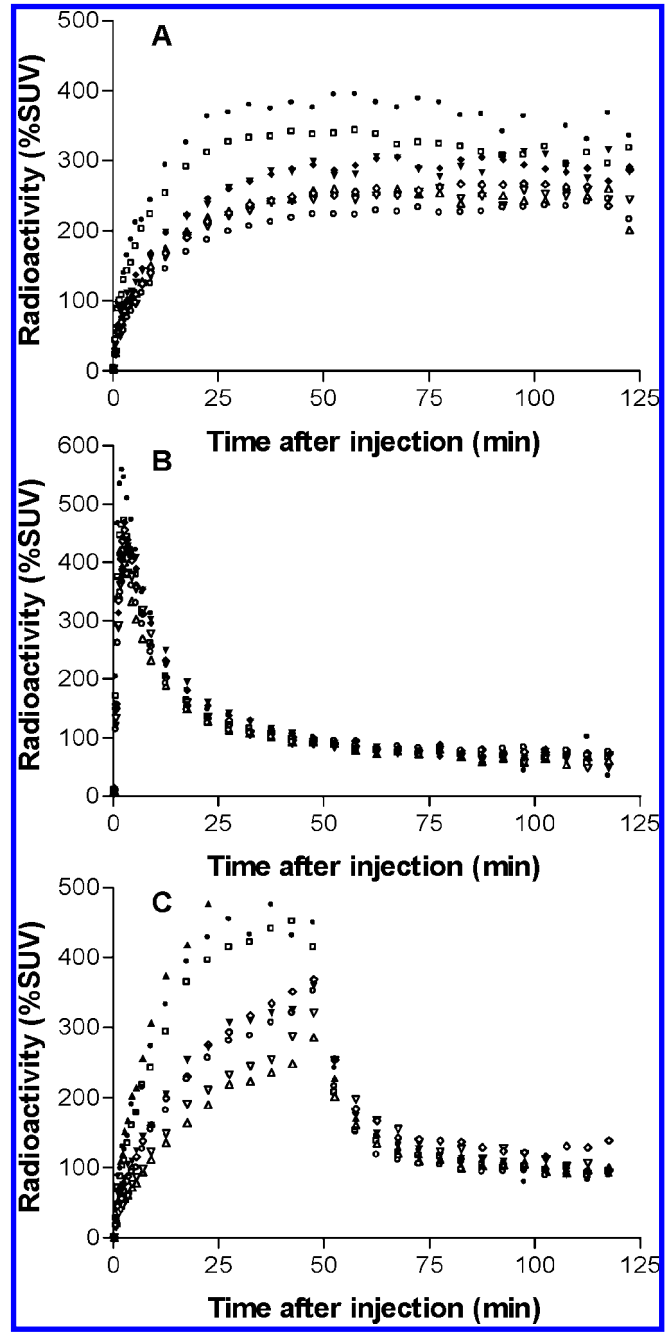

Figure 3. Brain region time-activity curves (TACs) in rhesus monkey after injection of [^{11}C]**10** alone (baseline experiment) (A), after injection of DAA1106 preceding [^{11}C]**10** at 24 min later (preblock experiment) (B), and after injection of [^{11}C]**10** and then PK 11195 at 45 min later (displacement experiment) (C). Experiments in parts A and B were performed in the same monkey (and the same monkey giving the data shown in parts A and B of Figure 2): □, cerebellum; △, occipital cortex; ▽, parietal cortex; ◇, temporal cortex; ○, frontal cortex; ◆, putamen; ▼, thalamus; ▲, striatum; ●, choroid plexus of fourth ventricle.

m/z 302 ([M + H − (CH_3 + $COOCH_3$)]$^+$) and 334 ([M + H − CH_2CO]$^+$) in its full scan MS. MS−MS analysis showed the product ions *m/z* 302 (100%) and *m/z* 334 (<10%). LC−MS of the acid **4** (t_R = 11.52 min) showed *m/z* 362 ([M + H]$^+$) and the fragment ions *m/z* 320 ([M + H − CH_2CO]$^+$) and 302 ([M + H − (CH_3 + COOH)]$^+$). MS−MS analysis gave the same ions (*m/z* 302, 100%). LC−MS of ligand **10** (t_R = 12.9 min) showed *m/z* 349 ([M + H]$^+$), and its dissociation in MS−MS analysis generated major product ions *m/z* 308, 307, 255, 188, and 121. LC−MS of **8** (t_R = 10.1 min) showed *m/z* 229 ([M + H]$^+$), and its dissociation yielded the product ions *m/z* 187 and 135. GC−MS of 2-methoxybenzoic acid **15** (t_R = 8.3 min) showed molecular ion *m/z* 152 and fragment ions *m/z* 135, 123, 105, 92, 79, 77, and 63.

Analysis of Rat Brain Extract after Ligand Injection. In an experiment in which ligand **3** was administered to rat, LC−MS analysis of brain extract acquired at 95 min showed a peak (t_R = 14.73 min) for the protonated molecule ([M + H]$^+$, *m/z* 376) and fragment ions *m/z* 334 and 302 assignable to unmetabolized **3**. In the total-ion current, a search for

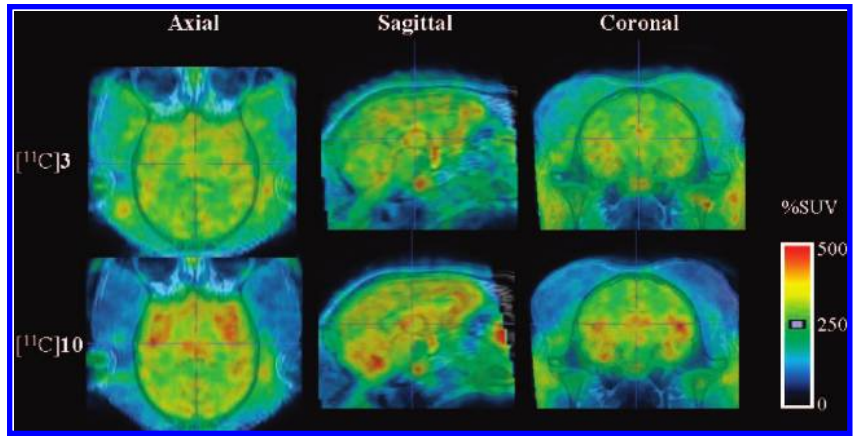

Figure 4. Axial, sagittal, and coronal PET summation images of monkey brain coregistered with MRI scans from (top row) a baseline experiment with [^{11}C]**3** and from (bottom row) a baseline experiment with [^{11}C]**10**. PET data are summed between 100 and 150 min and between 80 and 120 min for [^{11}C]**3** and [^{11}C]**10**, respectively.

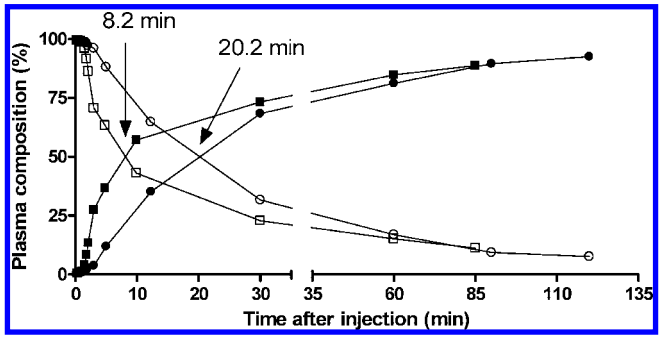

Figure 5. Time course of radioactivity composition in plasma after injecting [^{11}C]**3** into rhesus monkey, either alone (baseline experiment) or after coadministration with **3** (self-block experiment). The experiments were performed in the same monkey (and the same monkey producing the data shown in Figure 7): ○, parent [^{11}C]**3** in baseline experiment; ●, radiometabolite in baseline experiment; □, parent [^{11}C]**3** in self-block experiment; ■, radiometabolite in self-block experiment. The arrows give the times at which radioactivities in plasma are composed equally of parent radioligand and radiometabolite.

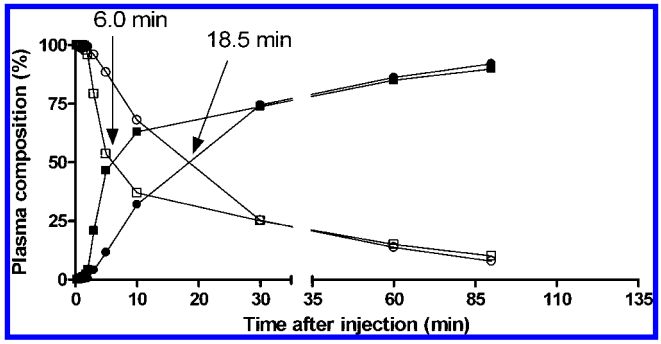

Figure 6. Time course of radioactivity composition in plasma after injecting [^{11}C]**10** into rhesus monkey, either alone (baseline experiment) or after pretreatment with DAA1106 (preblock experiment). The experiments were performed in the same monkey (and the same monkey producing the data shown in Figure 8): ○, parent [^{11}C]**10** in baseline experiment; ●, radiometabolite in baseline experiment; □, parent [^{11}C]**10** in preblock experiment; ■, radiometabolite in preblock experiment. The arrows give the times at which radioactivities in plasma are composed equally of parent radioligand and radiometabolite.

possible metabolite-specific ions (that might arise from ester hydrolysis, ring hydroxylation, deacetylation, or dealkylation) showed *m/z* 362 ([M + H]$^+$) along with a fragment ion *m/z* 302. The t_R for this component was 11.87 min. In addition,

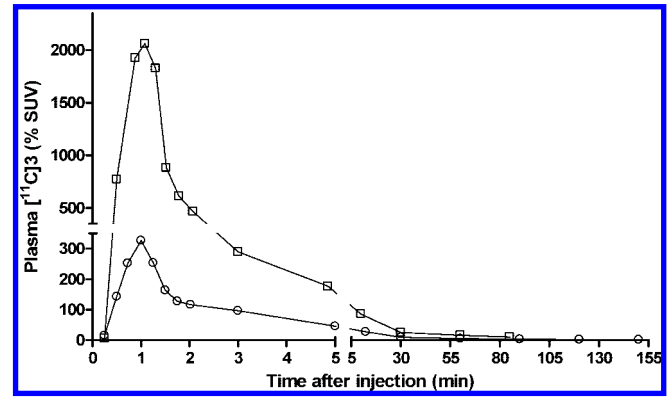

Figure 7. Time course of radioactivity (% SUV) in plasma represented by [^{11}C]**3** after injection into rhesus monkey under baseline conditions (○) and under self-block conditions (□).

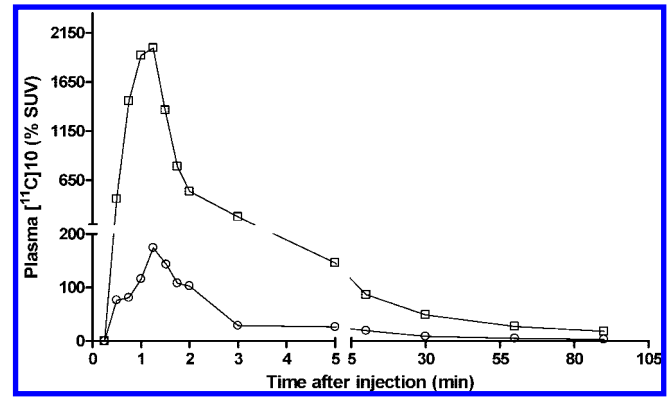

Figure 8. Time course of radioactivity (% SUV) in plasma represented by [^{11}C]**10** after injection into rhesus monkey under baseline condition (○) and under preblock condition (□).

MS−MS analysis showed product ions *m/z* 320 and 302 (100%). These LC−MS characteristics matched those of the acid **4**.

In the corresponding experiment with ligand **10**, LC−MS analysis of brain extract acquired at 120 min showed a peak at t_R = 12.9 min for [M + H]$^+$ (*m/z* 349) assignable to unmetabolized **10**. MS−MS analysis of this peak showed major product ions *m/z* 308, 307, 255, 188, and 121, confirming the presence of **10** in brain. The LC−MS screen for possible metabolites of **10** detected a compound (t_R = 10.2 min) with an intense [M + H]$^+$ ion (*m/z* 229) that gave fragment ions

Table 2. Radioactivity in Rat Plasma, Urine, and Brain Represented by Unchanged Radioligand at 30 min after Intravenous Administration

		radioactivity as unchanged radioligand (%)[a]		
radioligand	injected carrier (μg/kg)	plasma	urine	brain
[^{11}C]**3**	0.54	13.1 ± 1.0[b] (85.5 ± 1.4)[b]	nd[f]	83.0 ± 0.7[b] (86.9)
[^{11}C]**3**	2.96	3.4 ± 1.1[b] (91.6 ± 0.9)[b]	nd[f]	64.5, 64.5[c] (87.3)
[^{11}C]**10**	0.06	4.2[d]	nd[f]	97.6 [d]
[^{11}C]**10**	0.86	7.0, 7.0[c] (91.5, 91.6)[c]	nd[f]	94.4 ± 0.1[e] (81.2)
[^{11}C]**10**	4.83	2.4, 3.0[c] (85.3 ± 2.3)[b]	0.39 ± 0.01 (88.2 ± 8.2)[b]	89.1, 99.5[c] (92.3)

[a] The remainder of radioactivity was the single more polar radiometabolite in each case. Values shown in parentheses are recoveries of radioactivity from tissue into the analytical sample (%). [b] Mean ± SD from three HPLC analyses of one sample taken from one rat. [c] Values from two HPLC analyses of one sample taken from one rat. [d] Single determination. [e] Mean ± SD from four HPLC analyses of one sample taken from one rat. [f] nd = not determined.

m/*z* 187 and 135 in MS−MS. These LC−MS and MS−MS characteristics matched those of reference 4-phenoxy-3-acetylaminopyridine (**8**). No other metabolite was detected by LC−MS.

Analysis of Rat Urine after Ligand Injection. In the experiment in which ligand **3** was administered to rat, LC−MS analysis of collected urine showed a weak peak for $[M + H]^+$ (*m*/*z* 376) at $t_R = 14.74$ min. In addition, fragment ion *m*/*z* 302 was present at the same retention time. These LC−MS characteristics matched those of ligand **3**. The presence of **3** in urine was further confirmed by MS−MS analysis, which gave the same product-ion spectrum as **3**. The brain metabolite, **4**, was not detected in urine. Also, an extensive search with LC−MS failed to show any other possible urinary metabolites.

In the corresponding experiment with ligand **10**, only a low concentration of unmetabolized **10** appeared in urine. LC−MS did not detect the $[M + H]^+$ ion. However, more sensitive MS−MS showed a peak at $t_R = 12.9$ min with all the product ions of **10**. LC−MS did detect a peak at $t_R = 10.1$ min for *m*/*z* 229 ion corresponding to the $[M + H]^+$ ion of metabolite **8**. In addition, MS−MS of this peak showed all the product ions of metabolite **8**.

The metabolic N-debenzylation of **10**, while generating metabolite **8**, should also yield an equimolar amount of 2-methoxybenzaldehyde (**14**). Once generated, **14** is likely to be oxidized rapidly to 2-methoxybenzoic acid (**15**). To search for this possible metabolite, urine was extracted into ethyl acetate and analyzed by GC−MS with electron ionization detection. The ion chromatogram showed a molecular ion *m*/*z* 152 at $t_R = 8.3$ min. The fragment ions in the mass spectrum were *m*/*z* 135, 123, 105, 92, 79, 77, and 63. Reference **15** showed the same GC−MS and characteristics as this metabolite. Thus, metabolites **8** and **15** were both present in rat urine.

Discussion

Ligands **3** and **10** appeared attractive for development as potential PET radioligands for PBR because of their reported high affinities[45,46] and amenability to labeling with carbon-11 through simple reactions with [^{11}C]iodomethane. Moreover, their computed lipophilicities, as indexed by cLogP and cLogD values, are lower than the very high values of PK 11195 (cLogP = cLogD = 5.28) (Table 1). These properties of **3** and **10** were expected to be conducive to better brain entry, higher specific binding, and lower nonspecific binding in vivo than for PK 11195. Ligands **3** and **10** were readily synthesized in a few steps from commercially available materials according to described general methods (Schemes 1 and 2).[45,46] Each ligand was assayed for affinity to PBR through determination of K_i values in binding assays on human, rat, and monkey mitochondrial tissue with tritiated PK 11195 as radioligand. These assays showed that ligand **3** has somewhat higher affinity than ligand **10** for PBR in all three species (Table 1). The K_i values of **3** are comparable to those of the prototypical aryloxyanilide PBR ligand, DAA1106, and lower than the K_i values of PK 11195 in the same assays (Table 1). A small species-dependent variation in PBR affinity was evident for **3**, **10**, and DAA1106. Ligand **10** was found to show excellent PBR selectivity in a broad pharmacological screen run through the NIMH Psychoactive Drug Screening Program.

For use in ^{11}C-labeling, the acid precursor **4** to [^{11}C]**3** was obtained by simple hydrolysis of **3** (Scheme 1) and the phenol precursor **13** to [^{11}C]**10** by a simple three-step synthesis (Scheme 3). Both radioligands were easily prepared by alkylation with [^{11}C]iodomethane and obtained pure in adequate radiochemical yields and specific radioactivities. The LogD values for these radioligands were then determined experimentally and were in quite close agreement with those predicted by computation, again showing ligand **10** to have lower lipophilicity than **3**, with a value lying in the range that is generally considered desirable for achieving good brain entry.[47,48] The formulated radioligands were radiochemically stable and also stable in monkey plasma for at least 30 min. In monkey blood, each radioligand was found to be distributed similarly and heavily into cells (Table 1), consistent with the known cellular presence of PBR.[2] In accord with its lower lipophilicity, [^{11}C]**10** gave a significantly greater free fraction (f_P value) than [^{11}C]**3** (Table 1). The higher f_P value of **10** presents the considerable advantage of allowing its accurate measurement for input into potential biomathematical models.

Significant species differences in the brain distribution of PBR exist.[49] PBR are known by autoradiography in vitro to be present in the choroid plexus and cerebellum of rhesus monkey,[49] but little is known concerning their detailed distribution throughout the remainder of monkey brain. Other PBR radioligands (e.g., [^{11}C]DAA1106) have been observed by PET to have high uptake into the occipital cortex, olfactory bulb, and choroid plexus of rhesus monkey in vivo.[30,36]

After intravenous injection of [^{11}C]**3** into rhesus monkey, PET revealed a substantial initial uptake of radioactivity followed by slow washout from all selected volumes of interest (cerebellum, occipital cortex, parietal cortex, temporal cortex, frontal cortex, putamen, thalamus, and choroid plexus of the fourth ventricle) (Figure 2A). After 10 min from radioligand injection, the highest uptake (~250% SUV) was observed in the choroid plexus of the fourth ventricle and in the cerebellum and the lowest uptake in the frontal cortex. The selectivity of the brain radioactivity uptake for binding to PBR was tested in self-block and displacement experiments. In the self-block experiment, performed in the same monkey as in the baseline experiment, the uptake of radioactivity into all examined brain regions was fast and higher than in the baseline experiment and was then followed by a fast washout of radioactivity from all regions to the same very low level (Figure 2B). The higher initial uptake of radioactivity into brain is explained by the blockade of PBR

in peripheral organs, leading to a higher plasma level of radioligand, as confirmed by measurements in blood (see below). In the displacement experiment, administration of PK 11195 at 45 min after the radioligand caused a progressive reduction of radioactivity from all examined brain regions to a low level (~100% SUV) at 120 min (Figure 2C), thereby showing that the majority of radioactivity in brain was specifically bound to PBR before displacement. These data confirmed the high selectivity of the radioactivity in the brain for binding to PBR and also the relatively very low level of nonspecific binding in the baseline experiment.

The results obtained with PET for [^{11}C]**10** in monkey were similar to those for [^{11}C]**3** except that brain uptake of radioactivity in the baseline experiment was appreciably higher in the same monkey (Figure 3A). Maximal uptake was about 400% SUV in the choroid plexus of the fourth ventricle. This uptake far exceeds the uptake of [^{11}C]PK 11195 in normal rhesus monkey brain (maximum of about 130% SUV).[36] In the preblock experiment, with DAA1106 as blocking agent, the observed kinetics were similar to those in the self-block experiment with [^{11}C]**3**, again showing increased initial uptake of radioactivity and fast washout from all regions (Figure 3B). In another PET experiment, administration of PK 11195 at 45 min after radioligand resulted in a sharp decline of radioactivity from all examined brain regions to a low level, showing that the majority of radioactivity in brain had been bound to PBR (Figure 3C).

Each radioligand provided similar PET images of summed radioactivity distribution in brain in axial, sagittal, and coronal sections which, on coregistrations with MRI scans, matched with the limited previous information[30,36,49] on the regional distribution of PBR in rhesus monkey brain (Figure 4). Thus, high radioactivity uptake was seen in known PBR-rich regions such as cerebellum, occipital cortex, and choroid plexus of the fourth ventricle.

It is noted that the determination of the ratios of PBR specific binding to nonspecific binding achieved in monkey brain with either [^{11}C]**3** or [^{11}C]**10** cannot be assessed by simple inspection of the regional time-activity curves, since no reference region devoid of PBR that might represent nonspecific binding was identified. Moreover, the plasma input function of unchanged radioligand is highly dependent on the degree to which peripheral and brain PBR are occupied by carrier ligand or other blocking/displacing agent (see below); a peripheral blockade of [^{11}C]**10** binding to PBR in peripheral organs, such as kidney, spleen, and lungs, by PK 11195 has recently been demonstrated.[50] Full biomathematical analysis of brain data in conjunction with the measured plasma input function of unchanged radioligand is required to determine specific binding in any brain region. Such detailed analyses for [^{11}C]**3**[51] and [^{11}C]**10**[52] have revealed a very high level of specific binding (>90%) for these radioligands in monkey brain.

In monkey, [^{11}C]**3** was found to be almost completely metabolized to a single polar radioactive metabolite by 120 min (Figure 5). The time taken for radiometabolite in blood to equal parent radioligand was faster in the self-block experiment (8.2 min) than in the baseline experiment (20.2 min) (Figure 5). This difference might be explained by the higher level of parent radioligand in plasma in the self-block than in the baseline experiment during the early phase of the experiments (Figure 7), and therefore the greater early availability of parent radioligand to metabolizing enzymes.

In monkey, [^{11}C]**10** was also found to be metabolized to a single polar radiometabolite, which represented almost all radioactivity in plasma by 90 min. The time taken for radiometabolite to equal parent radioligand in plasma was faster in the preblock experiment (6.0 min) than in the baseline experiment (18.5 min) conducted in the same monkey (Figure 6). These findings again appear consistent with the much greater early level of parent radioligand in plasma in the preblock experiment than in the baseline experiment (Figure 8).

Experiments were performed in rats to obtain more detailed information on the metabolism of the two radioligands. Each radioligand was found to be metabolized to a single polar radiometabolite as in monkey. At 30 min after the injection of high specific radioactivity [^{11}C]**3** or [^{11}C]**10** into rats, the parent radioligand represented 13.1% or 4.2% of radioactivity in plasma, respectively (Table 2). These measures were appreciably lower (3.4% and 2.7%, respectively) when the radioligands were administered with much higher amounts of carrier ligand (Table 2). Again, a greater availability of the radioligands in plasma to metabolizing enzymes due to partial blockade of PBRs by the higher amounts of carrier may account for this difference. After administration of radioligand at high specific radioactivity (low carrier), the radioactivity in brain at 30 min was predominantly parent radioligand (83% for [^{11}C]**3** and 97.6% for [^{11}C]**10**) (Table 2). For radioligands administered at low specific radioactivity (high carrier) the percentage of radioactivity present as parent radioligand in brain was lower. This was especially so for [^{11}C]**3**. In three rats given [^{11}C]**10** with different carrier doses there was a clear trend of reduced amount of radiometabolite in brain with increased carrier dose. Even at very high carrier dose the proportion of radioactivity in brain represented by [^{11}C]**10** was high at 90%. The effect of increasing carrier on reducing the proportion of radioactivity in brain represented by parent radioligand was probably due to (i) less PBR-specific radioligand binding in brain and (ii) more rapid appearance of radiometabolite in plasma, each due to partial blockade of PBR. In one experiment with [^{11}C]**10**, in which the rat was perfused with saline during sacrifice, the composition of radioactivity in brain (97.8% [^{11}C]**10**) was similar to that expected in a nonperfused rat given the same amount of carrier. Hence, we conclude that radioactivity in blood did not greatly affect the measurements in nonperfused rats. In the high carrier experiment with [^{11}C]**10**, nearly all the radioactivity found in urine was radiometabolite (Table 2).

Experiments were performed in rats to elucidate the metabolic pathways of [^{11}C]**3** and [^{11}C]**10**. LC−MS and MS−MS analyses of rat brain extracts after intravenous administration of **3** detected **3** plus the acid **4** from its hydrolysis. In urine, only the parent ligand was detected. No metabolites from other conceivable routes of metabolism were detected in either brain or urine. The identified hydrolytic route of metabolism of **3**, acting on [^{11}C]**3**, would first give [^{11}C]methanol as radiometabolite, which would then be converted rapidly into [^{11}C]carbon dioxide and be expired. Hence, [^{11}C]**3** is not expected to give radiometabolite that might accumulate in the brain to confound accurate quantitation of PBR.

LC−MS and MS−MS analyses of rat brain extracts and urine after the administration of **10** detected **10** and also 4-phenoxy-3-acetylaminopyridine arising (**8**) from N-debenzylation. This route of metabolism has been observed for structurally related compounds, such as [^{18}F]FEDAA1106.[39] The N-debenzylation of [^{11}C]**10** should also give [^{11}C]2-methoxybenzaldehyde ([^{11}C]**14**) in equimolar amount to **8**. [^{11}C]**14** would be expected to be oxidized rapidly to [^{11}C]2-methoxybenzoic acid ([^{11}C]**15**) (Scheme 4). After the administration of **10** to rat, **15** was detected in urine, confirming N-debenzylation to be the main

Scheme 4. Metabolism of [^{11}C]**10** in Rat

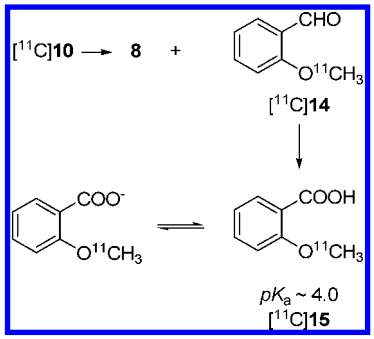

route of metabolism of **10**. [^{11}C]**15** would not be expected to accumulate in the brain because at physiological pH it will be almost fully ionized (p$K_a \approx 4.1$; ref 53) and have a very low LogD (calculated as −1.52). Moreover, we established that [^{11}C]**10** was stable in rat brain homogenate for 2 h, showing that radiometabolite was not generated in the brain but in the periphery. Hence, this radiometabolite should not prove to be troublesome for the quantitation of brain PBR with [^{11}C]**10**.

The findings on routes of metabolism in rats are not necessarily transferable to monkeys or humans. Nevertheless, since one single polar radiometabolite was found for each radioligand in rat and rhesus monkey, it is very likely that the same routes of metabolism occur in these species.

Conclusions

Both [^{11}C]**3** and [^{11}C]**10** showed more favorable properties than [^{11}C]PK 11195 for imaging PBR in monkey brain, including higher brain entry, higher PBR-specific signal, low nonspecific binding, and metabolism limited to the production of a single polar radiometabolite. Overall [^{11}C]**10** may be regarded as a marginally more promising PET radioligand than [^{11}C]**3** because of its superior brain entry, higher specific signal, and easily measurable free fraction in blood. This conclusion is also supported by rigorous kinetic analyses of [^{11}C]**3**[51] and [^{11}C]**10**.[52] [^{11}C]**10** is already beginning to find application in rats[54] and warrants further evaluation in human subjects, which is now in progress under an FDA-approved exploratory IND.

Experimental Section

Materials. Poly(ethyleneimine) and PK 11195 [1-(2-chlorophenyl)-*N*-methyl-*N*-(1-methylpropyl)-3-isoquinoline carboxamide] were purchased from Sigma (St. Louis, MO). DAA1106 (*N*-(2,5-dimethoxybenzyl)-*N*-(5-fluoro-2-phenoxyphenyl)acetamide) was synthesized from commercially available 2,5-difluoronitrobenzene according to the route described previously.[45] An ethanolic solution of [*N*-methyl-^{3}H]PK 11195 was purchased from Perkin-Elmer (Wellesley, MA) at a specific activity of 83.5 Ci/mmol. The radiochemical purity of [^{3}H]PK 11195 was verified to be >97% by instant thin layer chromatography (ITLC-SGl layers; Pall Gelman, East Hills, NY) with the use of three mobile phases ($CHCl_3$/MeOH, 95:5 v/v; EtOAc/hexane, 80:20 v/v; MeOH/H_2O/Et_3N, 97:3:0.1, by volume). [^{11}C](*R*)-PK 11195 was prepared via methylation of (*R*)-desmethyl-PK 11195 (from ABX, Radeberg, Germany) with [^{11}C]iodomethane (see below), essentially according to a previously described method[17]. Other chemicals were purchased from Aldrich Chemical Co. (Milwaukee, WI) and used as received. All animals used in this study were handled in accordance with the Guide for the Care and Use of Laboratory Animals[55] and the National Institute of Mental Health Animal Care and Use Committee. Human brain tissue was obtained from the Clinical Brain Disorders Branch, National Institute of Mental Health, and experiments with this material were performed under the regulations of the Ethics Committee of the National Institutes of Health.

General Methods. γ-Radioactivity from ^{11}C was measured with a calibrated dose calibrator (Atomlab 300, Biodex Medical Systems) or for low levels (<1 μCi) with a well-type γ-counter (model 1080 Wizard, Perkin-Elmer) having an electronic window set between 360 and 1800 keV. ^{3}H was measured with a liquid scintillation counter (Tri-Carb, Perkin-Elmer). ^{11}C radioactivity measurements were corrected for background and physical decay.

^{1}H NMR (400 MHz) and ^{13}C NMR (100 MHz) spectra were recorded at room temperature on an Avance-400 spectrometer (Bruker; Billerica, MA). Chemical shifts are reported in δ units (ppm) downfield relative to the chemical shift for tetramethylsilane. Abbreviations br, s, d, t, and m denote broad, singlet, doublet, triplet, and multiplet, respectively.

High-resolution mass spectra (HRMS) were acquired from the Mass Spectrometry Laboratory, University of Illinois at Urbana–Champaign (Urbana, IL), under electron ionization conditions using a double-focusing high-resolution mass spectrometer (Autospec, Micromass Inc.) with samples introduced through a direct insertion probe.

LC−MS (general method A) was performed on a LCQ Deca instrument (Thermo Fisher Scientific; Waltham, MA) equipped with a reverse-phase HPLC column (Synergi Fusion-RP, 4 μm, 150 mm × 2 mm, Phenomenex; Torrance, CA) The instrument was set up to perform electrospray ionization (spray voltage 5 kV, nitrogen sheath flow 65 units, auxiliary gas flow 10 units, capillary voltage 35 V, and capillary temperature 260 °C). In the full scan MS acquisition, the instrument was set up to detect ions *m*/*z* 150−750. For the characterization of synthesized compounds the column was eluted at 150 μL/min either isocratically or with a gradient of a combination of water/methanol/acetic acid (90:10:0.5 by volume) and methanol/acetic acid (100:0.5 v/v). For the analysis of parent ligand and metabolites extracted from biological material the LC column was equilibrated with 80% mobile phase A (10 mM aqueous $HCOONH_4$) and 20% mobile phase B [MeCN/H_2O, 90:10 v/v containing 10 mM $HCOONH_4$]. The extracted sample was injected into the LC−MS instrument and eluted at 150 μL/min with a mixture of 80% A and 20% B for 2 min followed by a linear gradient reaching 20% A and 80% B over 8 min which was then held for 6 min. The LC effluents were diverted from waste into the electrospray module of the LC−MS at 2.5 min after the start of each analysis. At the end of each run, the mobile-phase composition was returned to 80% A and 20% B at 250 μL/min over 1 min. The column was allowed to equilibrate for 3 min before the start of another analysis.

For LC−MS−MS (general method B), the molecular ion was isolated with 1.5 amu width and dissociated in the ion trap at a specific collision energy level.

GC−MS analyses (general method C) were performed on a Polaris Q instrument (Thermo Fisher Scientific Corp.) equipped with a capillary GC column (J & W DB-5MS, 30 m × 0.252 mm × 0.25 μm, Agilent Technologies). The helium flow rate was set at 1 mL/min, injector temperature to 220 °C, and transfer line to 250 °C. The sample was injected splitless (for 1 min) at a column temperature of 60 °C. After 1 min the temperature was increased to 180 °C at a rate of 20 °C/min and held at this temperature for 5 min. Subsequently, the column was returned to the initial temperature. A full scan acquisition (*m*/*z* 60−400) was performed in positive-ion, electron-ionization mode of operation. The source temperature of the mass spectrometer was 250 °C.

Analytical radio-HPLC of [^{11}C]**3** and [^{11}C]**10** plus their radiometabolites from samples of biological material (general method D) was performed on a Nova-Pak C18 column (4 μm, 100 mm × 8 mm, Waters Corp.) housed in a radial compression module (RCM 100). Mobile phases for the analyses consisted of MeOH/H_2O/Et_3N (80:20:0.1 by volume for [^{11}C]**3** and its metabolites and 75:25:0.1 by volume for [^{11}C]**10** and its metabolites) at a flow rate of 1.5 mL/min unless otherwise stated. That all radioactivity had eluted from the column during each analysis was shown by subsequent injection of methanol (2 mL) and observation that no more radioactivity was eluted. The same HPLC method was applied to determine the radiochemical purities of [^{11}C]**3** and [^{11}C]**10** preced-

ing lipophilicity determinations and for the determination of radiochemical stability in various media (see below).

Melting points were measured with a Mel-Temp manual melting point apparatus (Electrothermal, Fisher Scientific) and were uncorrected.

Methyl 2-Formylbenzoate (1).[56,57] To a solution of 2-carboxybenzaldehyde (4.0 g, 26.6 mmol) and potassium carbonate (11 g, 80 mmol) in acetone (50 mL) was added iodomethane (1.66 mL, 26.7 mmol) at room temperature. The mixture was refluxed under nitrogen for 4 h, cooled to room temperature, filtered, and concentrated. The residue was extracted into chloroform, washed successively with water, saturated sodium bicarbonate solution, and saturated brine, and then dried over magnesium sulfate to give **1** (3.4 g, 78%). Mp 50 °C. Lit. mp 50 °C.[56] ^{1}H NMR ($CDCl_3$): δ 3.98 (3H, s), 7.63−7.67 (2H, m), 7.92−7.99 (2H, m), 10.62 (1H, s). ^{13}C NMR ($CDCl_3$): δ 52.79, 128.44, 130.39, 132.41, 132.99, 134.44, 137.70, 166.77, 192.16. GC−MS *m/z* 165.05 $(M + H)^+$.

***N*-(2-Methoxycarbonylbenzyl)-2-phenoxyaniline (2).** A solution of **1** (0.89 g, 5.4 mmol) and 2-phenoxyaniline (1.0 g, 5.4 mmol) in methanol (6 mL) was stirred for 24 h at room temperature. Then sodium borohydride (0.76 g, 20 mmol) was added slowly and the mixture stirred for 1 h. Acetic acid (5% v/v, 16 mL, 14 mmol) was added dropwise to the mixture, which was then stirred at room temperature for 30 min and extracted thrice with ethyl acetate. The organic layers were combined, washed with saturated sodium bicarbonate solution and then brine, dried over magnesium sulfate, filtered, and concentrated in vacuo. Flash chromatography of the residue on silica gel (hexane/EtOAc, 97:3 v/v) gave **2** (1.17 g, 65%). Mp 72−74 °C. ^{1}H NMR ($CDCl_3$): δ 3.82 (3H, s), 4.73 (2H, s), 4.96 (1H, s br), 6.60−6.67 (2H, m), 6.83−7.08 (4H, m), 7.25−7.35 (4H, m), 7.44−7.49 (2H, m), 7.94 (1H, d, J = 7.7 Hz). ^{13}C NMR ($CDCl_3$): δ 46.44, 52.04, 112.01, 116.90, 117.13, 119.66, 122.57, 124.97, 126.97, 128.73, 128.82, 129.66, 131.11, 132.36, 140.29, 141.42, 142.87, 157.72, 167.72. LC−MS, *m/z* 334.14 $(M^+ + H)$. HRMS calcd for $C_{21}H_{20}NO_3$ $(M^+ + H)$, 334.1443; found, 334.1442.

***N*-Acetyl-*N*-(2-methoxycarbonylbenzyl)-2-phenoxyaniline (3).**[58] Acetyl chloride (0.26 g, 3.3 mmol) was slowly added to a solution of **2** (1.0 g, 3.0 mmol) and triethylamine (0.3 g, 3.0 mmol) in dichloromethane (5 mL) at 0 °C. The mixture was stirred for 1 h at room temperature, poured into water, and extracted with dichloromethane. The organic layers were combined and washed successively with hydrochloric acid (0.5 M), saturated sodium bicarbonate solution, and saturated brine, and then dried over magnesium sulfate and concentrated in vacuo. The crude product was purified with flash chromatography on silica gel (hexane/EtOAc, 70:30 v/v) to give **3** (0.98 g, 71%). Mp 80 °C. Lit. mp 78−80 °C.[45,58] ^{1}H NMR ($CDCl_3$): δ 1.98 (3H, s), 3.71 (3H, s), 5.19 (1H, d, J = 15.3 Hz), 5.50 (1H, d, J = 15.6 Hz), 6.83−7.41 (m, 11H), 7.62 (1H, d, J = 7.5 Hz), 7.78 (1H. d, J = 7.5 Hz). ^{13}C NMR ($CDCl_3$): δ 22.18, 49.48, 51.94, 118.39, 119.38, 123.31, 124.12, 126.95, 129.13, 129.75, 129.89, 130.10, 130.24, 130.31, 132.05, 133.11, 138.57, 153.49, 155.73, 167.81, 171.26. LC−MS, *m/z* 376.15 $(M + H)^+$. HRMS calcd for $C_{23}H_{21}NO_4$ $(M^+ + H)$, 376.1549; found, 376.1549. LC (Luna C-18 column, 5 μm, 10 mm × 250 mm, Phenomenex; MeCN/0.1 M $HCOONH_4$, 70:30 v/v; 2 mL/min; λ = 254 nm): t_R = 4.72 min, purity 100%.

***N*-Acetyl-*N*-(2-carboxybenzyl)-2-phenoxyaniline (4).** Compound **3** (0.40 g, 1.06 mmol) was treated with potassium hydroxide in methanol (5% w/v) at room temperature for 1 h. The mixture was concentrated in vacuo, poured into water, and extracted with ethyl acetate. The organic layers were combined, washed with hydrochloric acid (0.5 M), saturated sodium bicarbonate and saturated brine, and then dried over magnesium sulfate, filtered, and concentrated in vacuo. The crude product was purified by flash chromatography on silica gel to give **4** (0.33 g, 85%). Mp 142−144 °C. ^{1}H NMR ($CDCl_3$): δ 2.00 (3H, s), 5.07 (1H, d, J = 15.6 Hz), 5.42 (1H, d, J = 15.3 Hz), 6.85−7.46 (11H, m), 7.60 (d, 1H, J = 7.5 Hz), 7.88 (d, 1H, J = 7.5 Hz). ^{13}C NMR ($CDCl_3$): δ 22.09, 50.29, 118.60, 119.36, 123.53, 124.25, 127.23, 129.44, 129.88, 129.96, 130.02, 130.97, 132.52, 133.20, 138.60, 153.29, 155.67, 171.62, 172.18. LC−MS, *m/z* 362.13 $(M^+ + H)$. HRMS calcd for $C_{22}H_{20}NO_4$ $(M^+ + H)$, 362.1392; found, 362.1408.

4-Chloro-3-nitropyridine (5).[59] 4-Hydroxy-3-nitropyridine (5.0 g, 36 mmol) was added to a stirred slurry of phosphorus pentachloride (8.3 g, 40 mmol) and phosphoryl chloride (2 mL, 21.5 mmol) and held at 60 °C. The mixture solidified. The temperature was raised to 140 °C and held for 6 h. Volatile material was then removed in vacuo at room temperature and the residue poured onto ice–water. Sodium carbonate was added dropwise while maintaining the solution at 0 °C until the mixture was basic. The mixture was extracted with diethyl ether, and the organic layers were filtered through Celite and dried over magnesium sulfate. Evaporation of solvents at room temperature gave a residue of **5** (4.9 g, 86%) that was stored under nitrogen in a freezer preceding rapid use in the next step. ^{1}H NMR ($CDCl_3$): δ 7.65 (1H, d, J = 5.4 Hz), 8.80 (1H, d, J = 5.4 Hz), 9.24 (1H, s).

3-Nitro-4-phenoxypyridine (6).[46] To a solution of phenol (3.1 g, 33 mmol) in THF (10 mL) was added a solution (1 M) of potassium *tert*-butoxide (33 mmol) in THF (33 mL) at room temperature. Then a solution of **5** (4.9 g, 31 mmol) in THF (20 mL) was slowly added. The mixture was stirred for 1 h at room temperature and then poured into ice–water, extracted with ethyl acetate, washed with saturated brine, dried over magnesium sulfate, and finally concentrated. The residue was crystallized from pentane to give **6** (6.3 g, 93%). Mp 75 °C. Lit. mp 73−75 °C.[46] ^{1}H NMR ($CDCl_3$): δ 6.88 (1H, d, J = 5.7 Hz), 7.25−7.65 (5H, m), 8.65 (1H, d, J = 5.7 Hz), 9.24 (1H, s). ^{13}C NMR ($CDCl_3$): δ 111.90, 120.93, 126.75, 130.66, 136.75, 147.47, 152.74, 154.57, 158.24. LC−MS *m/z* 217.3 $(M^+ + H)$. HRMS calcd for $C_{11}H_9N_2O_3$ $(M^+ + 1)$, 217.0613; found, 217.0612.

4-Phenoxy-3-pyridinamine (7). In a 100 mL two-necked flask fitted with a reflux condenser were placed **6** (6.6 g, 31 mmol), iron powder (325 mesh, 5.2 g, 93 mmol), and aqueous ethanol (50%, 6 mL). The mixture was heated to boiling, and hydrochloric acid (37%, 0.35 mL) in aqueous ethanol (50%, 2 mL) was added slowly. The mixture was then refluxed for 3 h. Then the hot solution was made just alkaline by adding aqueous sodium hydroxide solution (0.5 M, 8 mL), cooled, and filtered over Celite. Solvent was evaporated off. The residue was dissolved in dichloromethane and washed with sodium bicarbonate solution. The organic layer was dried over magnesium sulfate and evaporated to dryness to give **7** as a dark-red oil (4.2 g, 74%). ^{1}H NMR ($CDCl_3$): δ 3.88 (2H, s), 6.57 (1H, d, J = 5.1 Hz), 7.05−7.10 (2H, m), 7.18−7.27 (1H, m), 7.37−7.45 (2H, m), 7.89 (1H, d, J = 5.4 Hz), 8.16 (1H, s). ^{13}C NMR ($CDCl_3$): δ 110.97, 119.89, 124.87, 130.10, 134.09, 138.06, 140.85, 151.10, 154.56. HRMS calcd for $C_{11}H_{11}N_2O$ $(M^+ + 1)$, 187.0871; found, 187.0864.

***N*-Acetyl-*N*-3-(4-phenoxy)pyridine (8).** Acetyl chloride (66 μL, 0.82 mmol) was added dropwise to a solution of **7** (0.14 g, 0.76 mmol) plus triethylamine (0.13 mL, 0.92 mmol) in CH_2Cl_2 (2 mL) cooled in a dry ice bath. The cold bath was removed and the solution stirred at room temperature for 1 h. Then the reaction mixture was concentrated under vacuum, and the residue was poured into water (10 mL) and extracted with AcOEt (2 × 10 mL). The combined organic layers were washed with saturated sodium bicarbonate solution and saturated brine, dried over $MgSO_4$, filtered, and concentrated under vacuum to obtain an oil that was purified on silica gel (hexane/AcOEt, 6:4 to 4:6) to provide **8** as fine needles (95 mg, 55%). Mp 74−76 °C. ^{1}H NMR ($CDCl_3$) δ 2.27 (3H, s), 6.59 (d, J = 5.56 Hz, 1H), 7.11 (d, J = 8.54 Hz, 2H), 7.3 (t, J = 7.44 Hz, 1H), 7.46 (t, J = 7.0 Hz, 2H), 7.69 (s, 1H), 8.19 (d, J = 5.52 Hz, 1H). ^{13}C NMR ($CDCl_3$): δ 24.60, 109.50, 120.70, 125.62, 125.97, 130.43, 142.77, 145.78, 153.06, 153.55, 168.22. LC−MS *m/z* 229 $(M + H)^+$.

***N*-(2-Methoxybenzyl)-4-phenoxypyridin-3-amine (9).** A mixture of **7** (0.8 g, 4.3 mmol) and 2-methoxybenzaldehyde (0.58 g, 4.3 mmol) in toluene (10 mL) was heated to reflux. A Dean–Stark trap was used to collect azeotropically removed water. After 24 h the mixture was cooled to room temperature and concentrated in vacuo to remove toluene. The residue was dissolved in methanol (20 mL) and cooled to 0 °C. Sodium borohydride (0.64 g, 17.2

mmol) was added portionwise. The mixture was then stirred for 1 h at room temperature with further additions of sodium borohydride until reaction was shown to be complete by TLC. Acetic acid (5%, 16 mL) was added dropwise to the mixture, which was then stirred at room temperature for 30 min and extracted thrice with ethyl acetate. The organic layers were combined, washed with saturated sodium bicarbonate solution and brine, dried over magnesium sulfate, filtered, and concentrated in vacuo. The residue was purified by flash chromatography on silica gel to give **9** as a red oil (1.2 g, 90%). ^{1}H NMR ($CDCl_3$): δ 3.83 (3H, s), 4.45 (2H, s), 4.68 (1H, br s), 6.53 (1H, d, $J = 5.4$ Hz), 6.87−6.95 (2H, m), 7.02−7.07 (m, 2H), 7.16−7.42 (m, 5H), 7.84 (1H, d, $J = 5.7$ Hz), 8.09 (1H, s). ^{13}C NMR ($CDCl_3$): δ 43.05, 55.28, 110.33, 110.38, 119.89, 120.57, 124.74, 126.54, 128.64, 128.93, 130.05, 130.11, 134.12, 135.70, 139.53, 151.02, 154.85, 157.44. LC−MS *m/z* 307.14 ($M^+ + H$). HRMS, calcd for $C_{19}H_{19}N_2O_2$ ($M^+ + H$), 307.1447; found, 307.1446.

***N*-(2-Methoxybenzyl)-*N*-(4-phenoxypyridin-3-yl)acetamide (10).**[46] Compound **9** (0.60 g, 20 mmol) was dissolved in glacial acetic acid (10 mL), and then acetic anhydride (1.9 mL, 20 mmol) was added dropwise at room temperature. The reaction mixture was stirred for 2 h at reflux. Acetic acid was removed under reduced pressure. Sodium hydroxide solution (1 M) was added to the residue and the product extracted with ethyl acetate (3 × 10 mL). The organic layers were combined, washed with cold water, dried over magnesium sulfate, filtered, and concentrated. The residue was purified by flash chromatography on silica gel (CH_2Cl_2/MeOH, 95:5 v/v) to give **10** (0.57 g, 84%). Mp 89−91 °C. Lit. mp 92.5–93.0 °C.[46] ^{1}H NMR ($CDCl_3$): δ 1.99 (3H, s), 3.59 (3H, s), 4.90 (1H, d, $J = 14.1$ Hz), 5.16 (1H, d, $J = 14.1$ Hz), 6.57 (1H, d, $J = 5.6$ Hz), 6.76 (1H, d, $J = 8.2$ Hz), 6.87−6.95 (m, 3H), 7.20−7.31 (2H, m), 7.38−7.45 (3H, m), 8.22 (1H, s), 8.29 (1H, d, $J = 5.6$ Hz). ^{13}C NMR ($CDCl_3$): δ 22.32, 46.10, 55.06, 110.21, 110.39, 120.57, 120.73, 124.76, 125.92, 128.76, 129.05, 130.31, 131.39, 150.45, 151.70, 153.33, 157.63, 160.84, 170.67. LC−MS 349.15 ($M^+ + H$). HRMS calcd for $C_{21}H_{21}N_2O_3$ ($M^+ + 1$), 349.1552; found, 349.1543. LC (Onyx C-18 column, 4.6 mm × 100 mm, Phenomenex; MeCN/0.01 M $HCOONH_4$, 30:70 v/v; 3 mL/min; $\lambda = 220$ nm): $t_R = 5.91$ min, purity 99.85%.

2-Acetoxybenzaldehyde (11). To a solution of salicylaldehyde (2.0 g, 16 mmol) in pyridine (10 mL) at 0 °C was added acetic anhydride (1.7 mL, 18 mmol). The mixture was stirred at room temperature overnight, poured into water, and extracted with ethyl acetate. The organic layers were combined, washed with water, hydrochloric acid (10%) and saturated brine, and then dried over magnesium sulfate, filtered, and concentrated to give **11** (2.5 g, 95%). ^{1}H NMR ($CDCl_3$): δ 2.39 (3H, s), 7.15−7.89 (4H, m), 10.1 (1H, s). ^{13}C NMR ($CDCl_3$): δ 20.78, 123.42, 126.06, 131.28, 134.61, 135.28, 151.10, 169.26, 188.83.

2-((4-Phenoxypyridin-3-ylamino)methyl)phenol (12). A mixture of **7** (2.0 g, 10 mmol) and **11** (1.76 g, 10 mmol) in toluene (10 mL) was heated to reflux. A Dean–Stark trap was used to collect the azeotropically removed water. After 24 h the mixture was cooled to room temperature and concentrated in vacuo to remove toluene. The residue was dissolved in methanol (20 mL) and cooled to 0 °C. Sodium borohydride (1.51 g, 40 mmol) was added portionwise, the ice-bath removed, and the solution stirred for 3 h at reflux. After dropwise addition of acetic acid (5%, 16 mL), the mixture was stirred at room temperature for 30 min and then extracted thrice with ethyl acetate. The organic layers were combined, washed with saturated sodium bicarbonate solution and brine, and then concentrated in vacuo. Methanol was added and the obtained precipitate filtered off and dried in vacuo to give **12** (0.78 g, 25%). Mp 186−187 °C (dec). ^{1}H NMR (DMSO-d_6): δ 4.35 (2H, d, $J = 8.4$ Hz), 5.91 (1H, t, $J = 8.4$ Hz), 6.54 (1H, d, $J = 6.8$ Hz), 6.74 (1H, t, $J = 7.2$ Hz), 6.83 (1H, d, $J = 8.1$ Hz), 7.02−7.26 (5H, m), 7.42−7.49 (2H, m), 7.70 (1H, d, $J = 5.4$ Hz), 7.86 (1H, s), 9.61 (1H, s). ^{13}C NMR (DMSO-d_6): δ 41.43, 111.12, 115.50, 119.21, 120.02, 125.00, 125.50, 128.13, 128.52, 130.66, 133.89, 136.02, 138.70, 150.28, 155.27, 155.66. LC−MS *m/z* 293.12 ($M^+ + H$). HRMS calcd for $C_{18}H_{17}N_2O_2$ ($M^+ + H$), 293.1290; found, 293.1279.

***N*-(2-Hydroxybenzyl)-*N*-(4-phenoxypyridin-3-yl)acetamide (13).** Compound **12** (0.3 g, 1 mmol) was refluxed with acetic anhydride (0.19 mL, 2 mmol) in acetic acid (3 mL) at reflux for 3 h. Solvent was removed under vacuum. The residue was basified with aqueous sodium hydroxide (1 M) and extracted with ethyl acetate. The organic layer was washed successively with water, saturated sodium bicarbonate solution, and brine, dried over magnesium sulfate, filtered, and concentrated. This crude product was treated with potassium hydroxide in methanol (5% w/v, 5 mL) at room temperature for 3 h. The mixture was concentrated in vacuo, poured into water, and extracted with ethyl acetate. The combined organic layers were washed successively with hydrochloric acid (0.5 M), saturated sodium bicarbonate solution and saturated brine, then dried over magnesium sulfate, filtered, and concentrated in vacuo to give **13** (0.21 g, 63%). Mp 131−133 °C. ^{1}H NMR ($CDCl_3$): δ 2.02 (3H, s), 4.81 (2H, s), 6.62−6.80 (5H, m), 6.94 (1H, d, $J = 8.1$ Hz), 7.19−7.29 (2H, m), 7.36−7.42 (2H, m), 8.30 (1H, m), 8.40 (1H, d, $J = 5.7$ Hz), 9.26 (1H, s). ^{13}C NMR ($CDCl_3$): δ 21.70, 50.81, 110.66, 117.78, 119.37, 120.72, 121.55, 126.29, 127.91, 130.39, 131.30, 150.90, 151.54, 152.74, 156.15, 160.61, 173.76. LC−MS *m/z* 335.1 ($M^+ + H$). HRMS calcd for $C_{20}H_{19}N_2O_3$ ($M^+ + H$), 335.1396; found, 335.1396.

Radiosynthesis of [^{11}C]Iodomethane. No-carrier-added [^{11}C]carbon dioxide (~1.4 Ci) was produced in a target of nitrogen gas (~225 psi) containing oxygen (1%) via the ^{14}N(p,α)^{11}C reaction induced by irradiation with a 16 MeV proton beam (45 μA) for 40 min from a PETrace cyclotron (GE; Milwaukee, WI). [^{11}C]Iodomethane was produced within a lead-shielded hot-cell from the [^{11}C]carbon dioxide via reduction to [^{11}C]methane and iodination with a MeI MicroLab apparatus (GE; Milwaukee, WI).

Radiosynthesis of [^{11}C]3. At about 3 min before the end of radionuclide production (ERP), the acid precursor **4** (1 mg, 3.0 μmol) was dissolved in DMF (80 μL). At 1 min before ERP this solution was treated with tetra-*n*-butylammonium hydroxide in methanol (1.0 M, 2.8 μL) and loaded into a 2 mL stainless steel loop[60] of a commercially available radiomethylation apparatus (Bioscan; Washington, DC) housed within a lead-shielded hot cell. The precursor was conditioned by passage of helium (12 mL/min) through the loop for 10 min. [^{11}C]Iodomethane was then swept into the loop in a stream (12 mL/min) of helium until radioactivity in the loop was maximized (about 4 min after release of [^{11}C]iodomethane from the MeI MicroLab apparatus). Radiomethylation was allowed to proceed for 5 min at room temperature. Crude [^{11}C]**3** was flushed from the loop in the HPLC mobile phase (2 mL, MeCN, 10 mM $HCOONH_4$, 65:35 v/v) and purified with HPLC on an Ultrasphere C-18 column (5 μm, 10 mm × 250 mm, Beckman) eluted with the mobile phase at 8 mL/min with the eluate monitored for radioactivity (pin diode, Bioscan) and absorbance at 254 nm (System Gold 166, Beckman). [^{11}C]**3** ($t_R = 4.8$ min) was collected, concentrated to dryness under reduced pressure and heat (80 °C), formulated in sterile physiological saline (0.9% w/v, 10 mL) containing ethanol (5% v/v), and finally passed through a sterile filter (0.2 μm pore size, Millex-GV, Millipore; Bedford, MA) into a sterile, pyrogen-free dose vial.

The radiochemical purity, SR, and chemical purity of formulated [^{11}C]**3** were assessed by analytical HPLC of a 0.1 mL aliquot on a C-18 Luna column (4.6 mm × 100 mm) eluted with MeCN/10 mM $HCOONH_4$ (70:30 v/v) at 2 mL/min, with eluate monitored for radioactivity (pin diode, Bioscan) and absorbance at 254 nm (System Gold 166, Beckman) (t_R of [^{11}C]**3** = 5.0 min).

Radiosynthesis of [^{11}C]10. At about 3 min before ERP, the phenol precursor **13** (1 mg, 3.0 μmol) was treated with tetra-*n*-butylammonium hydroxide in methanol (0.5 M, 4 μL). This solution was loaded into the loop of stainless steel tubing (internal volume, 2 mL) of a commercially available radiomethylation apparatus (Bioscan) housed within a lead-shielded hot cell. The loop was then conditioned by flushing with helium (12 mL/min) for 10 min. [^{11}C]Iodomethane was swept into the loop in a stream (12 mL/

min) of helium until radioactivity in the loop was maximized (about 4 min after release of [^{11}C]iodomethane from the MeI MicroLab apparatus). Radiomethylation was allowed to proceed for 3 min at room temperature. Crude [^{11}C]**10** was flushed from the loop with HPLC mobile phase (2 mL, MeCN:10 mM $HCOONH_4$, 47: 53, v/v) and purified with HPLC on a Luna C-18 column (10 μm, 10 mm × 250 mm, Phenomenex) eluted with mobile phase at 8 mL/min, with eluate monitored for radioactivity and absorbance at 254 nm. [^{11}C]**10** (t_R = 7.5 min) was collected, concentrated to dryness by rotary evaporation under reduced pressure and heat (80 °C), formulated in sterile physiological saline (0.9% w/v; 10 mL) containing ethanol (5% v/v), and finally passed through a sterile filter (0.2 μm pore size, Millex-GV, Millipore) into a sterile, pyrogen-free dose vial.

Specific radioactivity, chemical purity, and radiochemical purity of [^{11}C]**10** were assessed by HPLC of a 0.1 mL aliquot of formulated [^{11}C]**10** on a monolithic Onyx C-18 column (4.6 mm × 100 mm) eluted with MeCN/10 mM $HCOONH_4$ (30:70 v/v) at 6 mL/min with eluate monitored for radioactivity and absorbance at 220 nm (t_R of [^{11}C]**10** = 3.0 min).

Computation of cLogP and cLogD and Measurement of LogD. cLogP and cLogD (at pH 7.4) values for **3**, **10**, **15**, PK 11195, and DAA1106 were computed with the program Pallas 3.0 for Windows (CompuDrug; S. San Francisco, CA).

The initial radiochemical purities of samples of [^{11}C](*R*)-PK 11195, [^{11}C]**3**, and [^{11}C]**10** to be used in the determination of LogD values were measured with radio-HPLC (general method C). LogD values were then measured by mixing a solution of ^{11}C-labeled ligand (~300 μCi) in saline (17 μL) containing ethanol (5% w/v) with sodium phosphate buffer (0.15 M, pH 7.4, 17 mL). Aliquots (1 mL) were added to each of six tubes and extracted with *n*-octanol (that had been pre-equilibrated with the phosphate buffer) by vortexing for 1 min. Each tube was then centrifuged for 1 min, and the phases were separated. Samples of each phase (200 μL) were counted for radioactivity, as previously described,[61] except that each of the remaining aqueous phases was also submitted to radio-HPLC analysis (general method C) to obtain the proportion of radioactivity present as "unchanged radioligand". The latter was used to correct the γ counts to obtain the true radioligand counts (corrected $cpm_{aq\ phase}$). (Such a correction was not applied to the octanol phase, since the measurement of the relatively very high activity of this phase, due to the extracted lipophilic radioligand, would not be prone to significant error from a very minor level of radioactive impurity.) Two more tubes containing phosphate buffer (0.1 M) and radioligand also served as a storage medium, usually for the duration of the study (3−4 h), after which the radiochemical purity and specific concentration of the radioligand were assayed to assess radiochemical stability and adsorption to the tube, respectively. LogD was calculated as log($cpm_{organic\ phase}$/corrected $cpm_{aq\ phase}$).

Ligand Pharmacological Assay and Screen. Rat brain mitochondrial fraction was prepared as described previously.[62] Briefly, male Sprague-Dawley rats (300−450 g) were anesthetized by inhalation of isoflurane (5%) in oxygen and sacrificed by decapitation. Excised brain was quickly cooled over ice, weighed, and homogenized in cold sucrose solution (0.32 M) in HEPES buffer (10 mM, pH 7.4, 10 mL). The homogenate was centrifuged at 900*g* for 10 min at 4 °C. The supernatant was collected and then centrifuged at 9000*g* for 10 min. The resulting pellet was suspended in HEPES buffer (50 mM, pH 7.4, 10 mL) and then centrifuged at 12000*g* for 10 min at 4 °C. This pellet was suspended in HEPES buffer (50 mM, pH 7.4), distributed into aliquots each at a concentration of 160 mg/mL of the original brain tissue weight, and stored at −70 °C until use. Monkey mitochondrial fraction from frozen samples of the temporal and parietal lobes and human mitochondrial fraction from frozen brain tissue samples were prepared in the same manner.

Inhibition of [^{3}H]PK 11195 binding to the rat brain mitochondrial fraction by DAA1106, **3**, or **10** was assessed at 4 °C in HEPES buffer (50 mM, pH 7.4). [^{3}H]PK 11195 (70 × 10^3 dpm) in buffer (100 μL) was added to each of 11 borosilicate tubes (final concentration of radioligand, 0.38 nM). Different amounts of test ligand in buffer (100 μL) were placed in eight tubes. For determination of nonspecific binding to brain tissue, buffer (100 μL) containing the highest inhibitor concentration (set between 0.1 and 0.3 μM) was placed in the 9th tube, and for determination of nonspecific binding to the filter, buffer (900 μL) was placed in the 10th tube. Buffer (100 μL) was placed in the 11th tube for determination of total binding. Buffer (1.0 mL) alone was placed in a 12th tube to provide a measure of background radioactivity. The assay was initiated by adding mitochondrial fraction (800 μL) to all tubes except the 10th and 12th tubes. The mixtures were incubated for 2 h at 4 °C and then with a cell harvester (Brandel) rapidly filtered through a GF/B filter (Whatman) that had been presoaked with 0.5% polyethyleneimine and washed thrice with ice-cold buffer (3 mL). Radioactivity on each filter was counted. Triplicate curves (nine tubes per curve) were determined in each of two independent experiments. For each test compound, self-displacement of [^{3}H]PK 11195 with PK 11195 was used as a control. IC_{50} values were calculated with GraphPad Prism version 4.03 (GraphPad Software; San Diego, CA) with "one site competition" curve-fitting. K_i values were calculated according to the Cheng and Prusoff equation:[63]

$$K_i = \frac{IC_{50}}{1 + \frac{[L]}{K_D}}$$

where [L] is the concentration (0.38 nM) and K_D the equilibrium dissociation constant of the reference radioligand ([^{3}H]PK 11195). The latter was determined with "Scatchard analysis of homologous displacement" from multiple runs of PK 11195 with self-displacement in each tissue type.

Ligand **10** was also submitted to the National Institute of Mental Health Psychoactive Drug Screening Program (NIMH-PDSP) for assessment of binding affinity against a wide range of other receptors and binding sites ($GABA_A$ subtypes, $5\text{-}HT_{1A-E,2A-C,3,5A,6,7}$, $\alpha_{1A,1B,2A-C}$, β_{1-3}, κ opiate, D_{1-5}, DAT, SERT, NET, H_{1-4}, and M_{2-5}). Detailed assay protocols are available at the NIMH-PDSP Web site (http://pdsp.cwru.edu).

Monkey PET Imaging Experiments. Three male rhesus monkeys (*Macaca mulatta*, 9−15 kg) were used for these PET experiments, which were radioligand alone (baseline experiments), receptor block experiments, or radioligand displacement experiments. A single monkey was used for four of the experiments, namely, the baseline and block experiments with [^{11}C]**3** and [^{11}C]**10**. In the self-block experiment with [^{11}C]**3**, **3** (~1 mg/kg iv) was given with the radioligand, and in the preblock experiment with [^{11}C]**10**, the PBR-selective ligand DAA1106 (2.83 mg/kg iv) was given 24 min before the radioligand. Different monkeys were used for the two displacement experiments. In the displacement experiment with [^{11}C]**3**, PK 11195 (1 mg/kg) was given by bolus injection over 2 min at 45 min after radioligand injection, and in the displacement experiment with [^{11}C]**10**, PK 11195 (5 mg/kg) was given by bolus injection over 2 min at 45 min after radioligand injection. Displacing agents were prepared for administration in these experiments by dissolution in ethanol (1 mL) plus Cremophor EL (30 mg) and then dilution to 10 mL with saline for injection. For each PET experiment, the monkey was initially anesthetized with ketamine and then maintained under anesthesia with isoflurane (1.5−2.05%). An intravenous perfusion line, filled with saline (0.9% w/v), was used for bolus injection of [^{11}C]**3** (3.76−4.93 mCi; SR at time of injection, 2.04−3.73 Ci/μmol; injected mass of carrier 0.38−0.87 μg) or [^{11}C]**10** (5.03−7.49 mCi; SR at time of injection, 2.28−8.90 Ci/μmol; injected mass of carrier 0.20−1.14 μg). PET serial dynamic images were obtained on an Advance (GE Medical Systems) or HHRT (Siemens/CPS; Knoxville, TN) PET camera. Scans were obtained for up to 125 min in up to 33 frames. Decay-corrected time−activity curves (TACs) were obtained for irregular volumes of interest (VOIs), selected from frontal cortex, temporal cortex, parietal cortex, occipital cortex, striatum, thalamus, cerebellum, and choroids plexus on the fourth ventricle. Radioactivity was

normalized for injected dose and monkey weight by expression as percent standardized uptake value [% SUV = (% injected dose per gram) × (body weight in grams)].

MRI and Image Fusion. All monkeys had T1-weighted magnetic resonance imaging (TR/TE/x = 24 ms/3 ms/300), acquired on a 1.5-T Horizon instrument (General Electric Medical Systems; Waukesha, WI). PET and NMR images were coregistered with SPM2 software (Wellcome Department of Cognitive Neurology, London, U.K.).

Stability of Radioligand in Monkey Whole Blood and Rat Brain Homogenate In Vitro. [^{11}C]**3** or [^{11}C]**10** was incubated for 45 min in monkey whole blood (1 mL). A sample of whole blood (0.45 mL) was removed, added to acetonitrile (0.7 mL), and centrifuged. Then the supernatant liquid was analyzed by reverse-phase radio-HPLC (general method C) as described previously in detail.[64]

One healthy rat (472 g) was killed and the brain excised and placed on ice immediately. The brain was homogenized intermittently in 2-fold ice-cold saline (0.9% w/v). [^{11}C]**10** (0.5 mCi, 0.5 mL in formulation vehicle) was added to the brain homogenate and placed in a reciprocating water bath at 37 °C. The mixture was sampled (100 μL) after 2 h. The samples were deproteinated with MeCN, diluted in water, centrifuged, and analyzed with radio-HPLC as described above.

Binding of [^{11}C]3 and [^{11}C]10 to Monkey Plasma Proteins.[65] The radioligand was added to pooled monkey plasma (0.5 mL), placed at the top of an "Amicon" Centrifree filter, and filtered by ultracentrifugation at 5000*g*. All components of the filter units were counted for radioactivity to allow calculation of the percentage of radioligand bound to plasma proteins.

Analysis of Radiometabolites from Monkey Blood. During monkey PET scans, blood samples were drawn periodically from the femoral artery and collected in heparin-treated Vacutainer tubes. The samples were centrifuged, and the plasma was separated. A plasma sample of known volume (50–200 μL) was measured for radioactivity. Another sample of plasma of known volume (300−450 μL) was mixed with acetonitrile (0.7 mL) and then centrifuged. The supernatant liquid was analyzed by radio-HPLC (general method C) eluted at a flow rate of 2.0 mL/min. The composition of decay-corrected radioactivity in plasma, in terms of percentages of radioligand and radiometabolites, was calculated from the acquired data.

Analysis of Metabolites from Rat Plasma, Urine, and Brain. All radioligands used in these experiments were of >99.99% radiochemical purity. Rats (265–312 g) were placed under 1.5% isoflurane anesthesia and injected intravenously over 3 min with [^{11}C]**3** (0.995 mCi, SR = 2.42 Ci/μmol, carrier dose 0.54 μg/kg; or 1.43 mCi, SR = 682 mCi/μmol, carrier dose 2.96 μg/kg) or with [^{11}C]**10** (1.37 mCi, SR = 1.83 Ci/μmol, carrier dose 0.86 μg/kg; or 2.34 mCi, SR = 540 mCi/μmol, carrier dose 4.83 μg/kg; or 0.472 mCi, SR = 2.16 Ci/μmol, carrier dose 0.06 μg/kg). A blood sample (∼2 mL) was drawn at 30 min after each injection, and the rats were sacrificed by intravenous injection of a saturated solution of potassium chloride. The brain was excised, and for the experiment with [^{11}C]**10** a sample of urine (1.2 mL) was also withdrawn from the urinary bladder with a hypodermic needle. The brain from another rat that had been injected with [^{11}C]**10** (0.277 mCi, SR = 1.68 Ci/μmol, carrier dose 0.13 μg/kg) was excised after its perfusion with saline (0.9% w/v, 30 mL) until the perfusate ran clear and then analyzed as for other brain samples. Samples of plasma, urine, and brain were then prepared for HPLC analysis as follows.

Plasma was separated from cells by centrifugation of the blood sample at 1800*g* for 1.5 min, and three aliquots (100 μL for [^{11}C]**3** or 450 μL for [^{11}C]**10**) were each placed in acetonitrile (500 μL for [^{11}C]**3**, 700 μL for [^{11}C]**10**) along with added carrier (3 μg of **3** or 10 μg of **10**), mixed thoroughly, and centrifuged at 9400*g* for 2 min. Precipitates were counted for radioactivity to allow calculation of radioactivity recovery into supernatant liquids. Water (100 μL) was added to the supernatant liquid of each sample, which was further mixed thoroughly and counted for radioactivity.

In one experiment with [^{11}C]**10**, three urine samples (100 μL) were each placed in acetonitrile (700 μL) along with **10** (10 μg) and further processed for HPLC analysis in the same manner as plasma samples.

Excised brains were weighed, placed in acetonitrile (2 mL), and counted for radioactivity. Each brain was then homogenized along with carrier [**3** or **10**, ∼50 μg]. Water (0.5 mL) was then added, and the brain was further homogenized and centrifuged. Precipitates and supernatant liquids were counted for radioactivity.

The prepared samples of supernatant liquids from plasma, urine, and brain were each analyzed by reverse-phase radio-HPLC (general method D). Mobile phase flow rates were 2.0 and 1.5 mL/min for the analyses of radiometabolites from [^{11}C]**3** and [^{11}C]**10**, respectively.

Analysis of Rat Brain and Urinary Metabolites of 3 and 10 by LC−MS−MS and GC−MS. LC−MS and MS−MS data on reference compounds **3**, **4**, **8**, and **10** and GC−MS data on reference compound **15** were obtained by analysis of acetonitrile solutions (10 μg/mL) by general methods A, B, and C, respectively.

A Sprague-Dawley rat (261 g) was placed under anesthesia with 1.5% isoflurane in oxygen and injected through the penile vein over 9 min with **3** (1.4. mg) in 10% aqueous ethanol in saline (0.9% w/v, 0.9 mL) containing Cremophor EL (30 mg, BASF Ludwigshafen; Germany). The urethra was clamped, and every 30 min the rat was injected with saline (0.9% w/v, 0.1 mL). After 95 min the bladder was exposed and urine (2.0 mL) withdrawn. The rat was then sacrificed by injection of a saturated solution of potassium chloride. The brain was excised, placed in acetonitrile (3 mL), homogenized with a tissue Tearor (model 985–370, Biospec Products Inc.), added to water (0.5 mL), and rehomogenized. The homogenate was centrifuged at 9400*g* for 10 min and the clear supernatant liquid decanted off. The precipitate was rehomogenized with acetonitrile (3 mL) and water and centrifuged as before. The supernatant liquids were combined. Urine and brain extracts were stored at −70 °C for later LC−MS (general method A) and LC−MS−MS analysis (general method B). This procedure was repeated in a healthy rat (363 g) with injection of **10** (1.33 mg) over 3 min and exposure of the bladder after 2 h.

Stored urine samples (250 μL) were prepared for LC−MS analysis (general method A) and LC−MS−MS analysis (general method B) by centrifugation (10000*g*, 5 min). The supernatant liquid was transferred to an autosampler vial and a sample (2 μL) injected into the LC−MS instrument. The stored extract of brain in acetonitrile was prepared for LC−MS analysis (general methods A and B) by evaporation in a SpeedVac apparatus (model SPD 131 DDA, Thermo Fisher Scientific), reconstitution of the residue in acetonitrile−water (1:1 v/v, 200 μL), and centrifugation. A sample (8 μL) of the clear supernatant liquid was injected into the LC−MS instrument.

Stored urine samples (100 μL), from the experiment with **10** only, were also prepared for GC−MS analysis (general method C). First, they were treated in a glass tube with sodium hydroxide solution (0.1 M, 100 μL) at 50 °C for 30 min. Then each sample was cooled, acidified with acetic acid (20 μL), and extracted with ethyl acetate (2 mL). Following centrifugation (500*g*, 2 min), the organic layer was transferred to another tube. The aqueous layer was extracted once more, and the combined ethyl acetate extracts were evaporated to dryness. The residue was vortexed with ethyl acetate (200 μL) and water (30 μL). Then the organic layer was transferred to an autosampler vial. A sample (1 μL) was injected into the GC−MS instrument.

Stored rat brain extracts (1 mL) from the experiment with **10** were prepared for GC−MS analysis (general method C) by evaporation to dryness in a SpeedVac apparatus, mixing of the residue with ethyl acetate (300 μL) and water (50 μL), and finally centrifugation. A sample (1 μL) of the organic layer was analyzed.

The urinary and brain metabolites of **3** or **10** were analyzed with LC−MS (general method A) and MS−MS (general method B). The molecular ion was dissociated in the ion trap at a collision energy level of 24% (for **3** and metabolites) or 40% (for **10** and metabolites).

Acknowledgment. This study was supported by the Intramural Research Program of the National Institutes of Health, specifically the National Institute of Mental Health. We thank the NIH PET Department for fluorine-18 production and successful completion of the scanning experiments, PMOD Technologies for providing the image analysis software, and the NIMH Psychoactive Drug Screening Program (PDSP) for performing assays. The PDSP is directed by Bryan L. Roth, Ph.D., with project officer Jamie Driscol (NIMH), at the University of North Carolina at Chapel Hill (Contract NO1MH32004). We also thank Dr. Fabrice G. Siméon (NIMH) for useful contributions.

References

(1) Papadopoulos, V.; Baraldi, M.; Guilarte, T. R.; Knudsen, T. B.; Lacapère, J. J.; Lindemann, P.; Norenberg, M. D.; Nutt, D.; Weizman, A.; Zhang, M. R.; Gavish, M. Translocator protein (18 kDa): new nomenclature for the peripheral-type benzodiazepine receptor based on its structure and molecular function. *Trends Pharmacol. Sci.* **2006**, *27*, 402–409.

(2) Braestrup, C.; Albrechtsen, R.; Squires, R. F. High densities of benzodiazepine receptors in human cortical areas. *Nature* **1977**, *269*, 702–704.

(3) McEnery, M. W.; Snowman, A. M.; Trifletti, R. R.; Snyder, S. H. Isolation of the mitochondrial benzodiazepine receptor: association with the voltage dependent anion channel and the adenine nucleotide carrier. *Proc. Natl. Acad. Sci. U.S.A.* **1992**, *89*, 3170–3174.

(4) Olson, J. M. M.; Ciliax, B. J.; Mancini, W. R.; Young, A. B. Presence of peripheral-type benzodiazepine binding sites on human erythrocyte membranes. *Eur. J. Pharmacol.* **1988**, *152*, 47–53.

(5) Lacapère, J.-J.; Papadopoulos, V. Peripheral-type benzodiazepine receptor: structure and function of a cholesterol-binding protein in steroid and bile acid biosynthesis. *Steroids* **2003**, *68*, 569–585.

(6) Bernassau, J. M.; Reversat, J. L.; Ferrara, P.; Caput, D.; Le Fur, G. A 3D model of the peripheral benzodiazepine receptor and its implication in intra mitochondrial cholesterol transport. *J. Mol. Graphics* **1993**, *11*, 236–244.

(7) Papadopoulos, V.; Amri, H.; Li, H.; Boujrad, N.; Vidic, B.; Garnier, M. Target disruption of the peripheral-type benzodiazepine receptor gene inhibits steroidogenesis in the R2C Leydig tumor cell line. *J. Biol. Chem.* **1997**, *272*, 32129–32135.

(8) Papadopoulos, V. In search of the function of the peripheral-type benzodiazepine receptor. *Endocr. Res.* **2004**, *30*, 677–684.

(9) Verma, A.; Facchina, S. L.; Hirsch, D. J.; Song, S. Y.; Dillahey, L. F.; Williams, J. R.; Snyder, S. H. Photodynamic tumor therapy: mitochondrial benzodiazepine receptors as a therapeutic target. *Mol. Med.* **1998**, *4*, 40–45.

(10) Gavish, M.; Bachman, I.; Shoukrun, R.; Katz, Y.; Veenman, L.; Weisinger, G.; Weizman, A. Enigma of the peripheral benzodiazepine receptor. *Pharmacol. Rev.* **1999**, *51*, 629–650.

(11) Casellas, P.; Galiegue, S.; Basile, A. S. Peripheral benzodiazepine receptors and mitochondrial function. *Neurochem. Int.* **2002**, *40*, 475–486.

(12) Anholt, R. R.; De Souza, E. B.; Oster-Granite, M. L.; Snyder, S. H. Peripheral-type benzodiazepine receptors: autoradiographic localization in whole body sections of neonatal rats. *J. Pharmacol. Exp. Ther.* **1985**, *233*, 517–526.

(13) Lang, S. The role of peripheral benzodiazepine receptors (PBRs) in CNS pathophysiology. *Curr. Med. Chem.* **2002**, *9*, 1411–1415.

(14) Papadopoulos, V.; Lecanu, L.; Brown, R. C.; Han, Z.; Yao, Z. X. Peripheral-type benzodiazepine receptor in neurosteroid biosynthesis, neuropathology and neurological disorders. *Neuroscience* **2006**, *138*, 749–756.

(15) Benavides, J.; Fage, D.; Carter, C.; Scatton, B. Peripheral type benzodiazepine binding sites are a sensitive indirect index of neuronal damage. *Brain Res.* **1987**, *421*, 167–172.

(16) Camsonne, R.; Crouzel, C.; Comar, D.; Mazière, M.; Prenant, C.; Sastre, J.; Moulin, M. A.; Syrota, A. Synthesis of 1-(2-chlorophenyl)-*N*-[^{11}C]methyl-*N*-(1-methylpropyl)-3-isoquinoline carboxamide (PK 11195): a new ligand for peripheral benzodiazepine receptors. *J. Labelled Compd. Radiopharm.* **1984**, *21*, 985–991.

(17) Shah, F.; Hume, S. P.; Pike, V. W.; Ashworth, S.; McDermott, J. Synthesis of the enantiomers of [*N*-methyl-^{11}C]PK 11195 and comparison of their behaviours as radioligands for PK binding sites in rats. *Nucl. Med. Biol.* **1994**, *21*, 573–581.

(18) Venneti, S.; Lopresti, B. J.; Wiley, C. A. The peripheral benzodiazepine receptor (translocator protein 18 kDa) in microglia: from pathology to imaging. *Progr. Neurobiol.* **2006**, *80*, 308–322.

(19) Cagnin, A.; Brooks, D. J.; Kennedy, A. M.; Gunn, R. N.; Myers, R.; Turkheimer, F. E.; Jones, T.; Banati, R. B. In-vivo measurement of activate microglia in dementia. *Lancet* **2001**, *358*, 461–467.

(20) Cagnin, A.; Myers, R.; Gunn, R. N.; Lawrence, A. D.; Stevens, T.; Kreutzberg, G. W.; Jones, T.; Banati, R. B. In-vivo visualization of activated glia by [^{11}C](*R*)-PK 11195-PET following herpes encephalitis reveals projected neuronal damage beyond the primary focal lesion. *Brain* **2001**, *124*, 2014–2027.

(21) Debruyne, J. C.; Versijpt, J.; Van Laere, K. J.; De Vos, F.; Keppens, J.; Strijckmans, K.; Achten, E.; Slegers, G.; Dierckx, R. A.; Korf, J.; De Reuck, J. L. PET visualization of microglia in multiple sclerosis patients using [^{11}C]PK 11195. *Eur. J. Neurol.* **2003**, *10*, 257–264.

(22) Debruyne, J. C.; Van Laere, K. J.; Versijpt, J.; De Vos, F.; Eng, J. K.; Strijckmans, K.; Santens, P.; Achten, E.; Slegers, G.; Korf, J.; Dierckx, R. A.; De Reuck, J. L. Semiquantification of the peripheral benzodiazepine ligand [^{11}C]PK11195 in normal human brain and application in multiple sclerosis patients. *Acta Neurol. Bel.* **2002**, *102*, 127–135.

(23) De Vos, F.; Dumont, F.; Santens, P.; Slegers, G.; Dierckx, R.; De Reuck, J. High performance liquid chromatographic determination of [^{11}C]1-(2-chlorophenyl)-*N*-methyl-*N*-(1-methylpropyl)-3-isoquinoline carboxamide in mouse plasma and tissue and in human plasma. *J. Chromatogr., B* **1999**, *736*, 61–66.

(24) Pike, V. W.; Halldin, C.; Crouzel, C.; Barré, L.; Nutt, D. J.; Osman, S.; Shah, F.; Turton, D. R.; Waters, S. L. Radioligands for PET studies of central benzodiazepine receptors and PK (peripheral benzodiazepine) binding sites—current status. *Nucl. Med. Biol.* **1993**, *20*, 503–525.

(25) Greuter, H. N. J. M.; Van Ophemert, P. L. B.; Luurtsema, G.; Van Berckel, B. N. M.; Franssen, E. J. F.; Windhorst, B. D.; Lammertsma, A. A. Optimizing an online SPE-HPLC method for analysis of (*R*)-[^{11}C]1-(2-chlorophenyl)-*N*-methyl-*N*-(1-methylpropyl)-3-isoquinolinecarboxamide [(*R*)-[^{11}C]PK11195] and its metabolites in humans. *Nucl. Med. Biol.* **2005**, *32*, 307–312.

(26) Lockhart, A.; Davis, B.; Matthews, J. C.; Rahmoune, H.; Hong, G.; Gee, A.; Earnshaw, D.; Brown, J. The peripheral benzodiazepine receptor ligand PK 11195 binds with high affinity to the acute phase reactant α1-acid glycoprotein: implications for the use of the ligand as a CNS inflammatory marker. *Nucl. Med. Biol.* **2003**, *30*, 199–206.

(27) Wala, E. P.; Sloan, J. W.; Jing, X. Pharmacokinetics of the peripheral benzodiazepine receptor antagonist, PK 11195, in rats. The effect of dose and gender. *Pharmacol. Res.* **2000**, *42*, 461–468.

(28) Gillings, N. M.; Bender, D.; Falborg, L.; Marthi, K.; Mun, O. L.; Cumming, P. Kinetics of the metabolism of four PET radioligands in living minipigs. *Nucl. Med. Biol.* **2001**, *28*, 97–104.

(29) Petit-Taboué, M.-C.; Baron, J.-C.; Barré, L.; Travère, J.-M.; Speckel, D.; Camsonne, R.; Mackenzie, E. T. Brain kinetics and specific binding of [^{11}C]PK 11195 to ω_3 sites in baboons: positron emission tomography study. *Eur. J. Pharmacol.* **1991**, *200*, 346–351.

(30) Zhang, M. R.; Ogawa, M.; Maeda, J.; Ito, T.; Noguchi, J.; Kumata, K.; Okauchi, T.; Suhara, T.; Suzuki, K. [2-^{11}C]Isopropyl-, [1-^{11}C]ethyl-, and [^{11}C]methyl-labeled phenoxyphenylacetamide derivatives as positron emission tomography ligands for the peripheral benzodiazepine receptor; radiosynthesis, uptake and in vivo binding in brain. *J. Med. Chem.* **2006**, *49*, 2735–2742.

(31) Kropholler, M. A.; Boellard, R.; Schuitemaker, A.; Folkersma, H.; van Berckel, B. N. M.; Lammertsma, A. A. Evaluation of reference tissue models for the analysis of [^{11}C](*R*)-PK11195 studies. *J. Cereb. Blood Flow Metab.* **2006**, *26*, 1431–1441.

(32) Turkheimer, F. E.; Edison, P.; Pavese, N.; Roncaroli, F.; Anderson, A. N.; Hammers, A.; Gerhard, A.; Hinz, R.; Tai, Y. F.; Brooks, D. J. Reference and target region modeling of [^{11}C]-(*R*)-PK11195 brain studies. *J. Nucl. Med.* **2007**, *48*, 158–167.

(33) Schuitemaker, A.; van Berkel, B. N. M.; Kropholler, M. A.; Veltman, D. J.; Scheltens, P; Jonker, C.; Lammertsma, A. A.; Boellaard, R. SPM analysis of prarametric (*R*)-[^{11}C]PK11195 binding images; plasma inoput versus reference tissue parametric methods. *NeuroImage* **2007**, *35*, 1473–1479.

(34) James, M. L.; Selleri, S.; Kassiou, M. Developement of ligands for the peripheral benzodiazepine receptor. *Curr. Med. Chem.* **2006**, *13*, 1991–2001.

(35) Zhang, M. R.; Kida, T.; Noguchi, J.; Furutsuka, K.; Maeda, J.; Suhara, T.; Suzuki, K. [^{11}C]DAA1106: radiosynthesis and in vivo binding to peripheral benzodiazepine receptors in mouse brain. *Nucl. Med. Biol.* **2003**, *30*, 513–519.

(36) Maeda, J.; Suhara, T.; Zhang, M. R.; Okauchi, T.; Yasuno, F.; Ikoma, Y.; Inaji, M.; Nagai, Y.; Takano, A.; Obayashi, S.; Suzuki, K. Novel peripheral benzodiazepine receptor ligand [^{11}C]DAA1106 for PET: an imaging tool for glial cells in brain. *Synapse* **2004**, *52*, 283–291.

(37) Probst, K. C.; Izquierdo, D.; Bird, J. L. E.; Brichard, L.; Franck, D.; Davies, J. R.; Fryer, T. D.; Richards, H. K.; Clark, J. C.; Davenport, A. P.; Weissberg, P. L.; Warburton, E. A. Strategy for improved [^{11}C]DAA1106 radiosynthesis and in vivo peripheral benzodiazepine receptor imaging using microPET, evaluation of [^{11}C]DAA1106. *Nucl. Med. Biol.* **2007**, *34*, 439–446.

(38) Zhang, M. R.; Maeda, J.; Furutsuka, K.; Yoshida, Y.; Ogawa, M.; Suhara, T.; Suzuki, K. [^{18}F]FMDAA1106 and [^{18}F]FEDAA1106: two positron-emitter labeled ligands for peripheral benzodiazepine receptor (PBR). *Bioorg. Med. Chem. Lett.* **2003**, *13*, 201–204.

(39) Zhang, M.-R.; Maeda, J.; Ogawa, M.; Noguchi, J.; Ito, J.; Yoshida, Y.; Okauchi, T.; Obayashi, S.; Suhara, T.; Suzuki, K. Development of a new radioligand, *N*-(5-fluoro-2-phenoxyphenyl)-*N*-(2-[^{18}F]fluoroethyl-5-methoxybenzyl)acetamide, for PET imaging of peripheral benzodiazepine receptor in primate brain. *J. Med. Chem.* **2004**, *47*, 2228–2235.

(40) James, M. L.; Fulton, R. R.; Henderson, D. J.; Eberl, S.; Meikle, S. R.; Thomson, S.; Allan, R. D.; Dolle, F.; Fulham, M. J.; Kassiou, M. Synthesis and in vivo evaluation of a novel peripheral benzodiazepine receptor PET radioligand. *Bioorg. Med. Chem.* **2005**, *13*, 6188–6194.

(41) Belloli, S.; Moresco, R. M.; Mataresse, M.; Biella, G.; Sanvito, F.; Simonelli, P.; Turolla, E.; Olivieri, S.; Cappelli, A.; Vomero, S.; Galli-Kienle, M.; Fazio, F. Evaluation of three quinoline-carboxamide derivatives as potential radioligands for the in vivo pet imaging of neurodegeneration. *Neurochem. Int.* **2004**, *44*, 433–440.

(42) Gulyas, B.; Halldin, C.; Vas, A.; Banati, R. B.; Shchukin, E.; Finnema, S.; Tarkainen, J.; Tihanyi, K.; Szilagyi, G.; Farde, L. [^{11}C]Vinpocetine; a prospective peripheral benzodiazepine receptor ligand for primate PET studies. *J. Neurol. Sci.* **2005**, *229*, 219–223.

(43) Ikomo, Y.; Yasuno, F.; Iti, H.; Suhara, T.; Ota, M.; Toyama, H.; Fujimara, Y.; Takano, A.; Maeda, J.; Zhang, M. R.; Nakao, R.; Suzuki, K. Quantitative analysis for estimating binding potential of the peripheral benzodiazepine receptor with [^{11}C]DAA1106. *J. Cereb. Blood Flow Metab.* **2007**, *27*, 173–184.

(44) Fujimara, Y.; Ikoma, Y.; Yasuno, F.; Suhara, T.; Ota, M.; Matsumoto, R.; Nozaki, S.; Takano, A.; Kosaka, J.; Zhang, M.-R.; Nakao, R.; Suzuki, K.; Kato, N.; Ito, H. Quantitative analyses of ^{18}F-FEDAA 1106 binding to peripheral benzodiazepine receptors in living human brain. *J. Nucl. Med.* **2006**, *47*, 43–50.

(45) Okubo, T.; Yoshikawa, R.; Chaki, S.; Okuyama, S.; Nakazato, A. Design, synthesis and structure−affinity relationships of aryloxyanilide derivatives as novel peripheral benzodiazepine receptor ligands. *Bioorg. Med. Chem.* **2004**, *12*, 423–438.

(46) Nakazato, A.; Okubo, T.; Nakamura, T.; Chagi, S.; Tomisawa, K.; Nagamine, M.; Yamamoto, K.; Harade, K.; Yoshida, M. Aryloxy Nitrogen-Containing Heteroarylamines Derivative, Their Use and MDR Ligands Containing Them. *JP Patent*, 001476, 2000. (in Japanese).

(47) Pike, V. W. Positron-emitting radioligands for studies in vivo—probes for human psychopharmacology. *J. Psychopharmacol.* **1993**, *7*, 139–158.

(48) Waterhouse, R. N. Determination of lipophilicity and its use as a predictor of blood−brain barrier penetration of molecular imaging agents. *Mol. Imaging Biol.* **2003**, *5*, 376–389.

(49) Cymerman, U.; Pazos, A.; Palacios, J. M. Evidence for species differences in "peripheral" benzodiazepine receptors: an autoradiographic study. *Neurosci. Lett.* **1986**, *66*, 153–158.

(50) Brown, A. K.; Fujita, M.; Fujimara, Y.; Liow, J.-S.; Stabin, M.; Ryu, Y. H.; Imaizumi, M.; Hong, J.; Pike, V. W.; Innis, R. B. Radiation dosimetry and biodistribution in monkey and man of ^{11}C-PBR28, a PET radioligand to image inflammation. *J. Nucl. Med.* **2007**, *48*, 2072–2079.

(51) Imaizumi, M.; Briard, E.; Zoghbi, S. S.; Gourley, J. P.; Hong, J.; Musachio, J. L.; Gladding, R.; Pike, V. W.; Innis, R. B.; Fujita, M. Kinetic evaluation in nonhuman primates of two new PET ligands for peripheral benzodiazepine receptors in brain. *Synapse* **2007**, *61*, 595–605.

(52) Imaizumi, M.; Briard, E.; Zoghbi, S. S.; Gourley, J. P.; Hong, J.; Fujimara, Y.; Pike, V. W.; Innis, R. B.; Fujita, M. Brain and whole-body imaging in non-human primates of [^{11}C]PBR-28, a promising radioligand for peripheral benzodiazepine receptors. *NeuroImage* **2007**, doi:10.1016/j.neuroimage.2007.09.063.

(53) Yasuda, M.; Yamasaki, K.; Ohtaki, H. Stability of complexes of several carboxylic acids formed with bivalent metals. *Bull. Chem. Soc. Jpn.* **1960**, *33*, 1067–1070.

(54) Imaizumi, M.; Kim, H.-J.; Zoghbi, S. S.; Briard, E.; Hong, J.; Musachio, J. L.; Ruetzler, C.; Chuang, D.-M.; Pike, V. W.; Innis, R. B.; Fujita, M. PET imaging with [^{11}C]PBR28 can localize and quantify upregulated peripheral benzodiazepine receptors associated with cerebral ischemia in rat. *Neurosci. Lett.* **2007**, *411*, 200–205.

(55) Clark, J. D.; Baldwin, R. L.; Bayne, K. A.; Brown, M. J.; Gebhart, G. F.; Gonder, J. C.; Gwathmey, J. K.; Keeling, M. E.; Kohn, D. F.; Robb, J. W.; Smith, O. A.; Steggerda, J.-A. D.; VandeBer, J. L. *Guide for the Care and Use of Laboratory Animals*; National Academy Press: Washington, DC, 1996.

(56) Osuka, A.; Nakajima, S.; Maruyama, K. Synthesis of 1,2-phenylene-bridged triporphyrin. *J. Org. Chem.* **1992**, *57*, 7355–7359.

(57) Ye, B.-H.; Naruta, Y. A novel method for the synthesis of regiospecifically sulfonated porphyrin monomers and dimers. *Tetrahedron* **2003**, *59*, 3593–3601.

(58) Nakazato, A.; Okubo, T.; Nakamura, T.; Shigeyuki, C.; Kazuyuki, T.; Nagamine, M.; Yamamoto, K.; Harada, K.; Yoshida, M. Heterocycle Substituted Aryloxyaniline Derivatives and Their Uses as MDR Ligands. U.S. Patent 6,476,056 B2, 2002.

(59) Stavenger, R. A.; Cui, H.; Dowdell, S. E.; Franz, R. G.; Gaitanopoulos, D. E.; Goodman, K. B.; Hilfiker, M. A.; Ivy, R. L.; Leber, J. D.; Marino, J. P., Jr.; Oh, H.-J.; Viet, A. Q.; Xu, W.; Ye, G.; Zhang, D.; Zhao, Y.; Jolivette, L. J.; Head, M. S.; Semus, S. F.; Elkins, P. A.; Kirkpatrick, R. B.; Dul, E.; Khandekar, S. S.; Yi, T.; Jung, D. K.; Wright, L. L.; Smith, G. K.; Behm, D. J.; Doe, C. P.; Bentley, R.; Chen, Z. X.; Hu, E.; Lee, D. Discovery of aminofurazan−azabenzimidazoles as inhibitors of rho-kinase with high kinase selectivity and antihypertensive activity. *J. Med. Chem.* **2007**, *50*, 2–5.

(60) Wilson, A. A.; Garcia, A.; Jin, L.; Houle, S. Radiotracer synthesis from [^{11}C]-iodomethane: a remarkably simple captive solvent method. *Nucl. Med. Biol.* **2000**, *27*, 529–532.

(61) Zoghbi, S. S.; Baldwin, R. M.; Seibyl, J. S.; Charney, D. S.; Innis, R. B. A radiometric technique for determining apparent pK_a of receptor binding ligands. *J. Labelled Compd. Radiopharm.* **1997**, *40* (Suppl. 1), 136.

(62) Chaki, S.; Funakoshi, T.; Yoshikawa, R.; Okuyama, S.; Okubo, T.; Nakazato, A.; Nagamine, M.; Tomisawa, K. Binding characteristics of [^{3}H]DAA1106, a novel and selective ligand for peripheral benzodiazepine receptors. *Eur. J. Pharmacol.* **1999**, *371*, 197–204.

(63) Cheng, Y.-C.; Prusoff, W. H. Relationship between the inhibition constant (K_i) and the concentration of inhibitor which causes 50% inhibition (IC_{50}) of an enzymatic reaction. *Biochem. Pharmacol.* **1973**, *22*, 3099–3108.

(64) Zoghbi, S. S.; Shetty, H. U.; Ichise, M.; Fujita, M.; Imaizumi, M.; Liow, J.-S.; Shah, J.; Musachio, J. L.; Pike, V. W.; Innis, R. B. PET imaging of the dopamine transporter with [^{18}F]FECNT: a polar radioactive metabolite confounds brain activity measurements. *J. Nucl. Med.* **2006**, *47*, 520–527.

(65) Gandelman, M. S.; Baldwin, R. M.; Zoghbi, S. S.; Zea-Ponce, Y; Innis, R. B. Evaluation of ultrafiltration for the free-fraction determination of single photon emission computed tomography (SPECT) radiotracers: β-CIT, IBF, and iomazenil. *J. Pharm. Sci.* **1994**, *83*, 1014–1019.

JM0707370